Report 9, 1992

STEAM GATHERING SYSTEM FOR THE NE-OLKARIA GEOTHERMAL FIELD, KENYA - PRELIMINARY DESIGN

Peter Ayodo Ouma,
UNU Geothermal Training Programme,
Orkustofnun - National Energy Authority,
Grensasvegur 9,
108 Reykjavik,
ICELAND

Permanent address:
Olkaria Geothermal Project,
P.O. Box 785,
Naivasha,
KENYA

ABSTRACT

The Northeast Olkaria geothermal field occupies an area of 12 km^2. It is one of three sectors which together form the Greater Olkaria geothermal field, located about 125 km northwest of Nairobi and situated within the East African Rift Valley. The other two sectors are the East and the West Olkaria geothermal fields. Production drilling is nearly complete with 27 wells already drilled in this sector. The developmental process is approaching the Detailed Design Stage. Due to environmental reasons it has been decided to reinject the effluent obtained from separation stations and from the cooling towers. The reinjection operation will involve pumping of the effluent to the reinjection well(s).

The objective for this study was to design a steam gathering system which would provide an efficient arrangement for collecting the effluent at a pumping station before being pumped to the reinjection well(s). The gathering system has been looked at in terms of cost operational convenience. The two-phase lay-out has been carefully selected ensuring that the flow is always downhill. In sizing the two-phase pipelines, the superficial steam velocity has been restricted to between 20 and 40 m/s and slug flow regime has been avoided. Two-phase pressure drop calculations have been done using two correlations, one by Lockhart-Martinelli and the other by Friedel. The sizing of major equipment that constitutes the system has been done. The calculated operational wellhead pressures are possible as seen from the output curves of the wells. The study has shown that it is possible to design a central separation system for utilizing the steam from the field. The total cost of the equipment required for the gathering system has been estimated at approximately USD 13 million.

TABLE OF CONTENTS

Page

LIST OF FIGURES

LIST OF TABLES

1. INTRODUCTION

The Northeast Olkaria geothermal field is one of the three sectors which together form the Greater Olkaria geothermal field, located about 125 km northwest of Nairobi and situated within the East African Rift Valley. The other two sectors are the East and the West Olkaria geothermal fields.

Exploration drilling in Olkaria started in 1974 leading to commencement of the development of East Olkaria in 1978. East Olkaria geothermal field has been producing electrical power since 1981 when the first 15 MW_e Unit started operation. The other two 15 MW_e Units came on line in 1982 and 1985, respectively, bringing the plant capacity to the current level of 45 MW_e. Concurrent with the development of the East Olkaria well field, exploration drilling was carried out in other sectors of the Greater Olkaria geothermal field. This exploration activity has been successful and has delineated two new areas for development. These are the Northeast and the West Olkaria geothermal fields (Figure 1).

The Northeast Olkaria geothermal field, occupying an area of as much as 12 km^2, is currently under development (June 1992). Production drilling is nearly complete with 27 wells already drilled in this sector. The developmental process is approaching the Detailed Design Stage. Due to environmental reasons it has been decided to reinject the effluent obtained from separation station(s) and from the cooling towers. The reinjection operation will involve pumping of the effluent to the reinjection well(s). In order to realize this it will be necessary to design a steam gathering system which will provide an efficient arrangement for collecting the effluent at the pumping station(s) before being pumped to reinjection well(s). The system should be economic and at the same time offer the most efficient use of the output from the production wells. The work described below is an attempt to achieve this objective. Some of the material given below has already been published (Ouma, 1992) and therefore for further details refer to that paper.

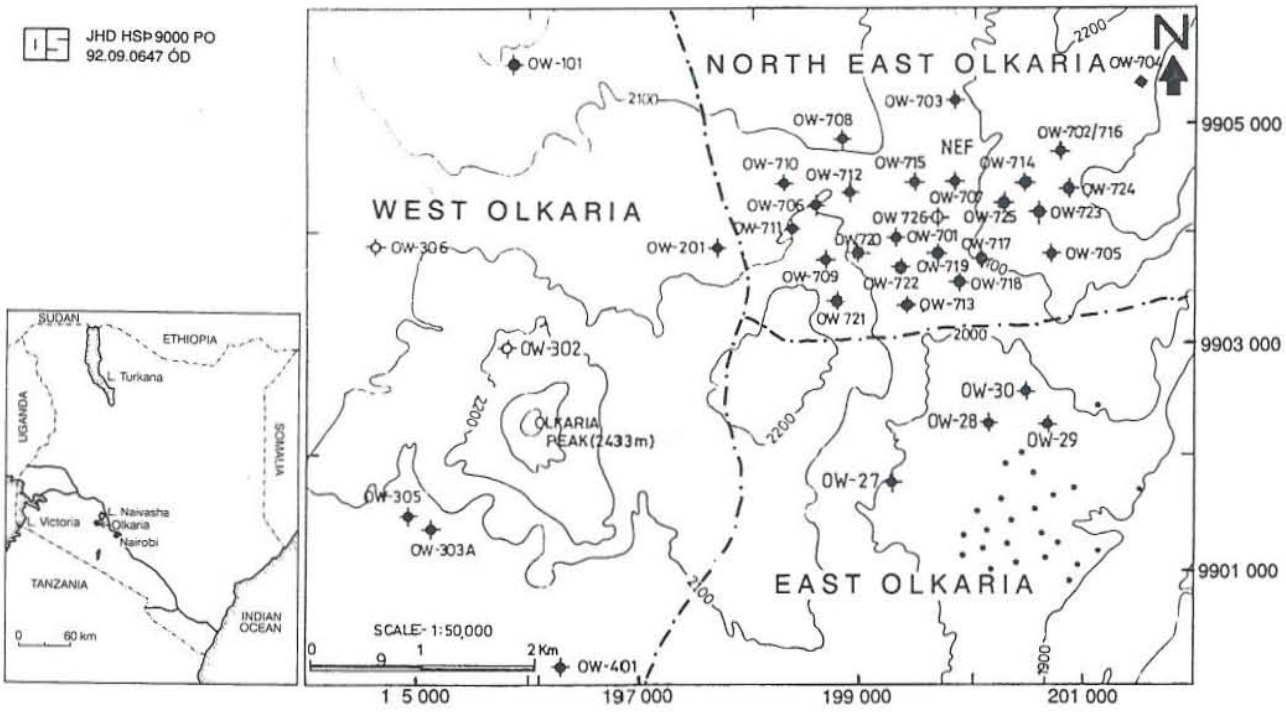

FIGURE 1: The location of the NE-Olkaria geothermal field, Kenya

2. AN OVERVIEW OF THE NE-OLKARIA GEOTHERMAL FIELD

2.1 Geological structure

The Olkaria geothermal field is associated with the Olkaria volcanic centre. The geothermal reservoir is considered to be bounded by arcuate faults forming a ring - or a caldera structure. The magmatic heat source is represented by intrusions at deep levels inside the ring structure. Faults and fractures are prominent in the area, particularly in West Olkaria. The general trend is N-S and E-W but there are also some inferred faults striking almost NW-SE (Figure 2).

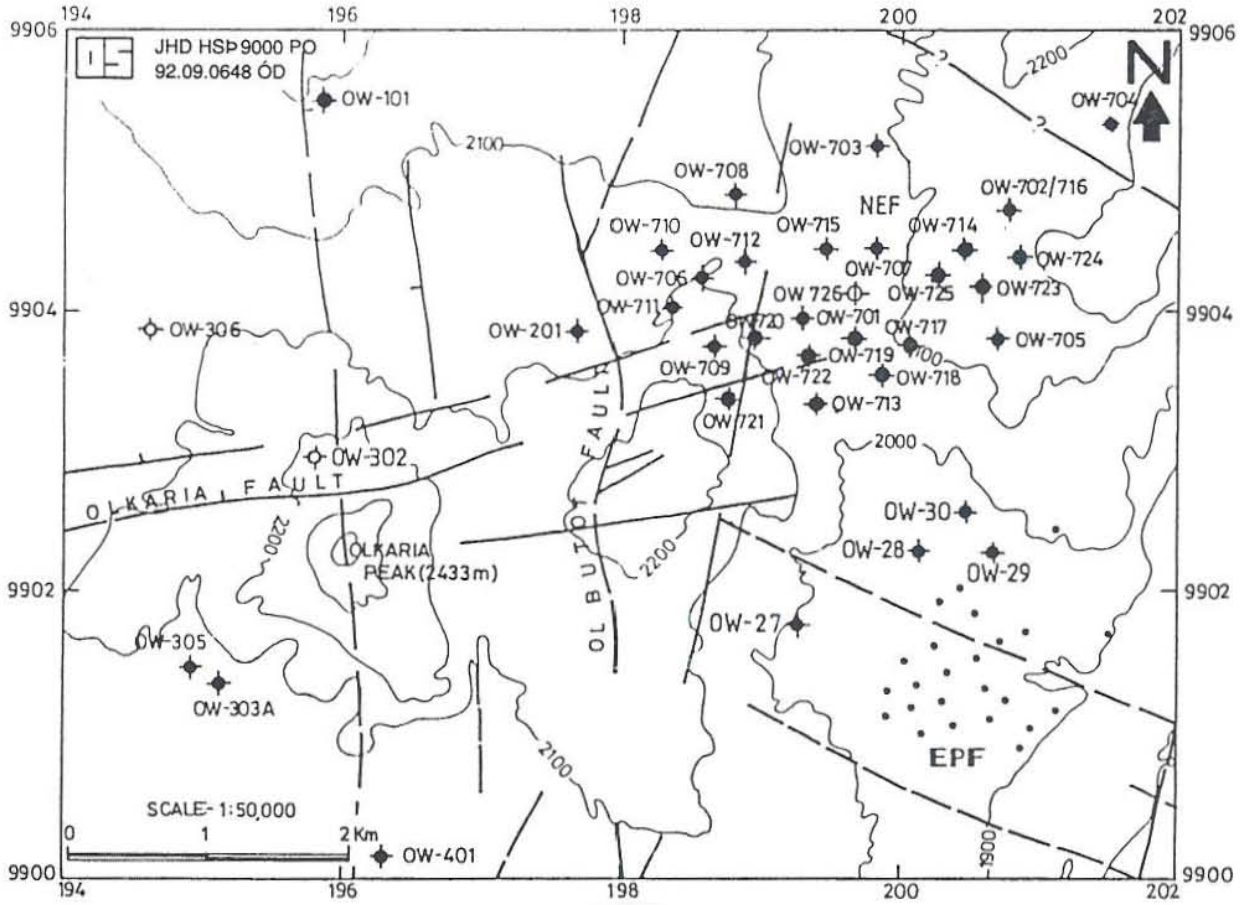

FIGURE 2: Geological structures of the Olkaria geothermal field

2.2 Temperature and pressure distribution

Extensive downhole measurements have been done in the NE-Olkaria field and Figures 3 and 4 show the stable temperature profiles for some wells there. Planar view of the temperature distribution in the field as obtained from stable downhole conditions at elevations 500, 750, 1075 and 1250 m a.s.l. are shown in Figures 5-8. The temperatures in the field are generally high with most wells attaining over 300°C at depths below 200 m a.s.l. The temperature distribution seems to suggest a structural control within the centre of the field which is probably the eastern extension of Olkaria fault. The observed temperature distribution corresponds to an upflow of hot

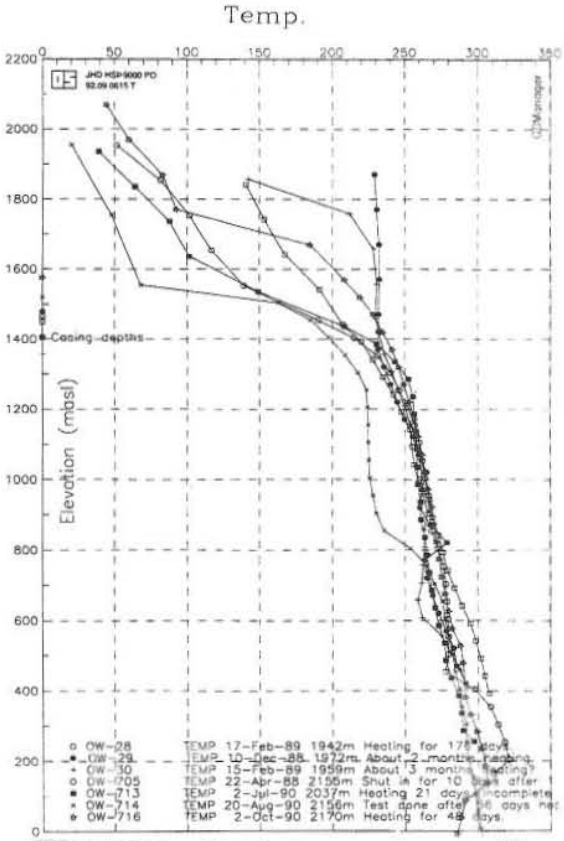

FIGURE 3: Stable temperature profiles in the south sector of NE-Olkaria

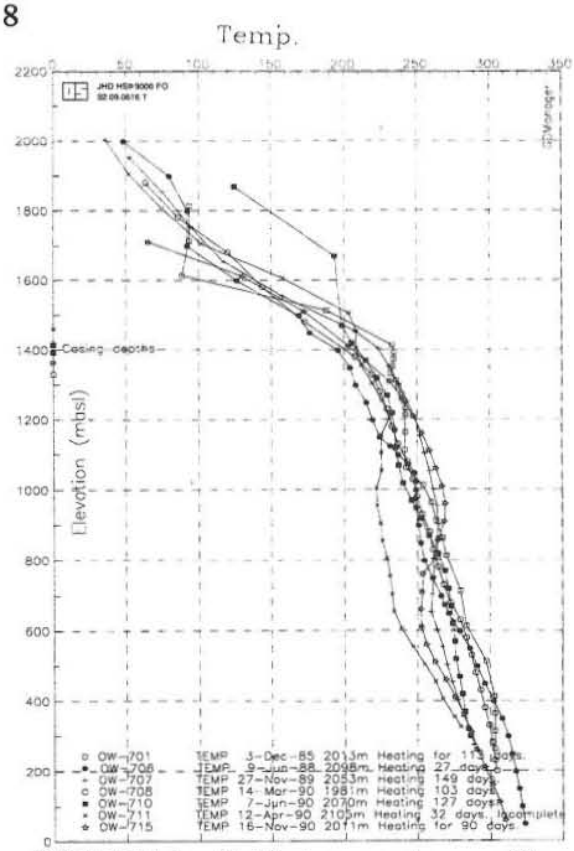

FIGURE 4: Stable temperature profiles in the north sector of NE-Olkaria

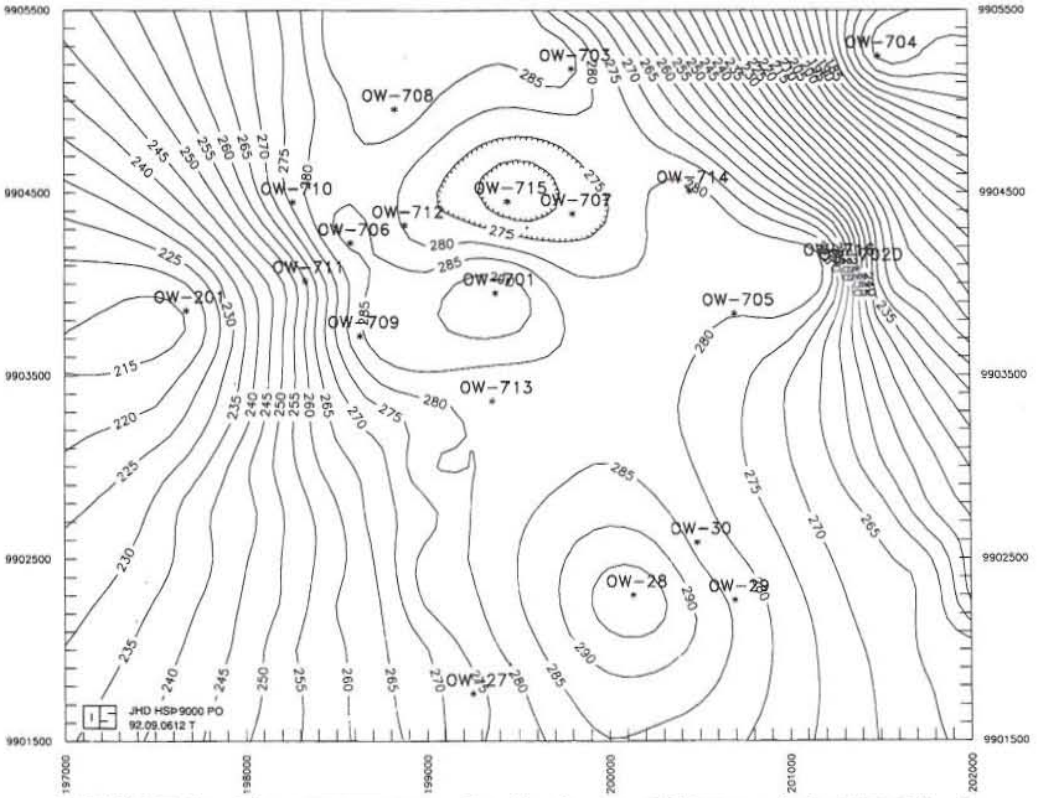

FIGURE 5: The temperature distribution at 1250 m a.s.l. in NE-Olkaria

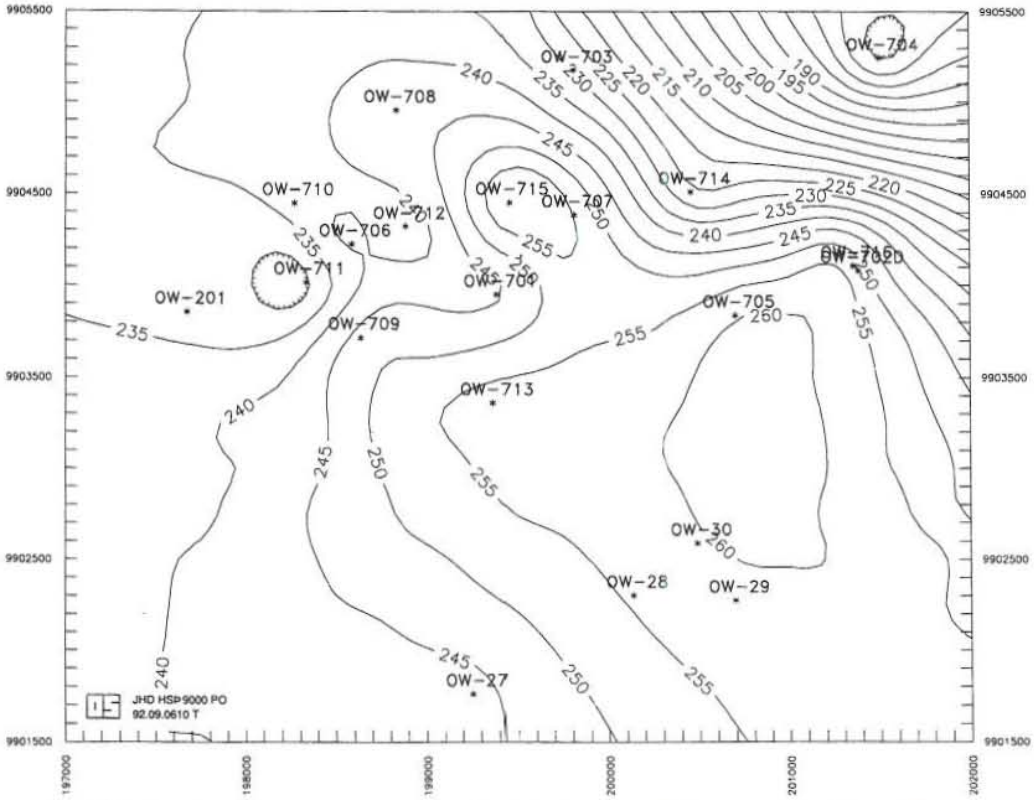

FIGURE 6: The temperature distribution at 1075 m a.s.l. in NE-Olkaria

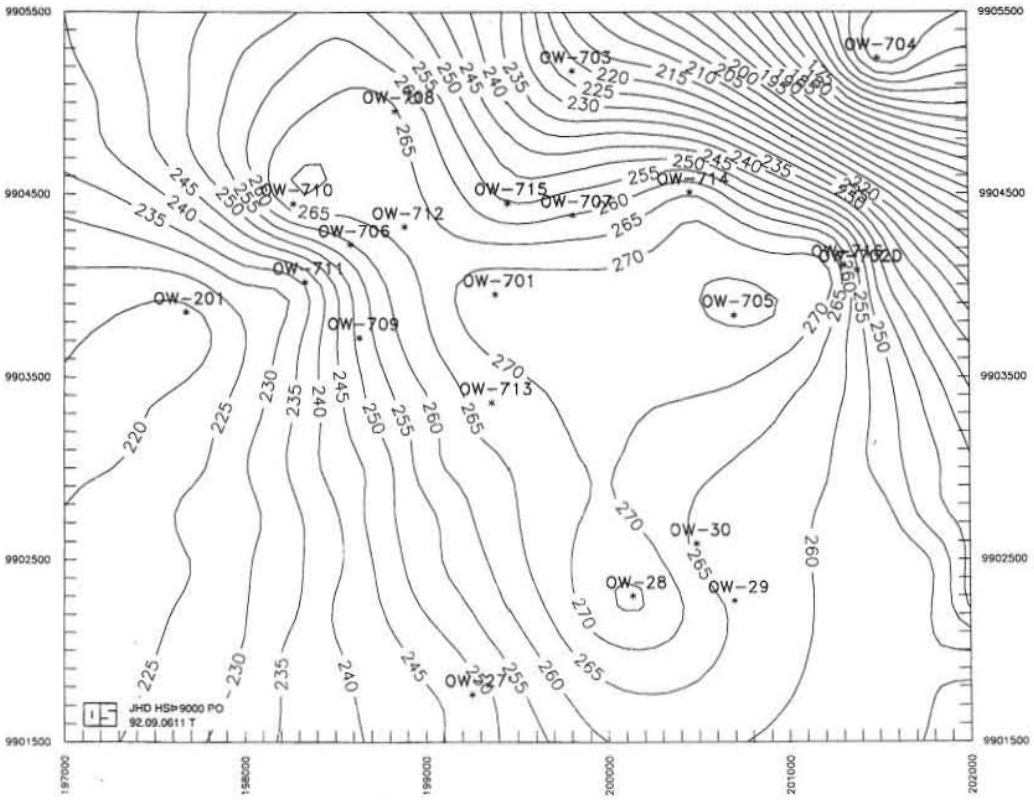

FIGURE 7: The temperature distribution at 750 m a.s.l. in NE-Olkaria

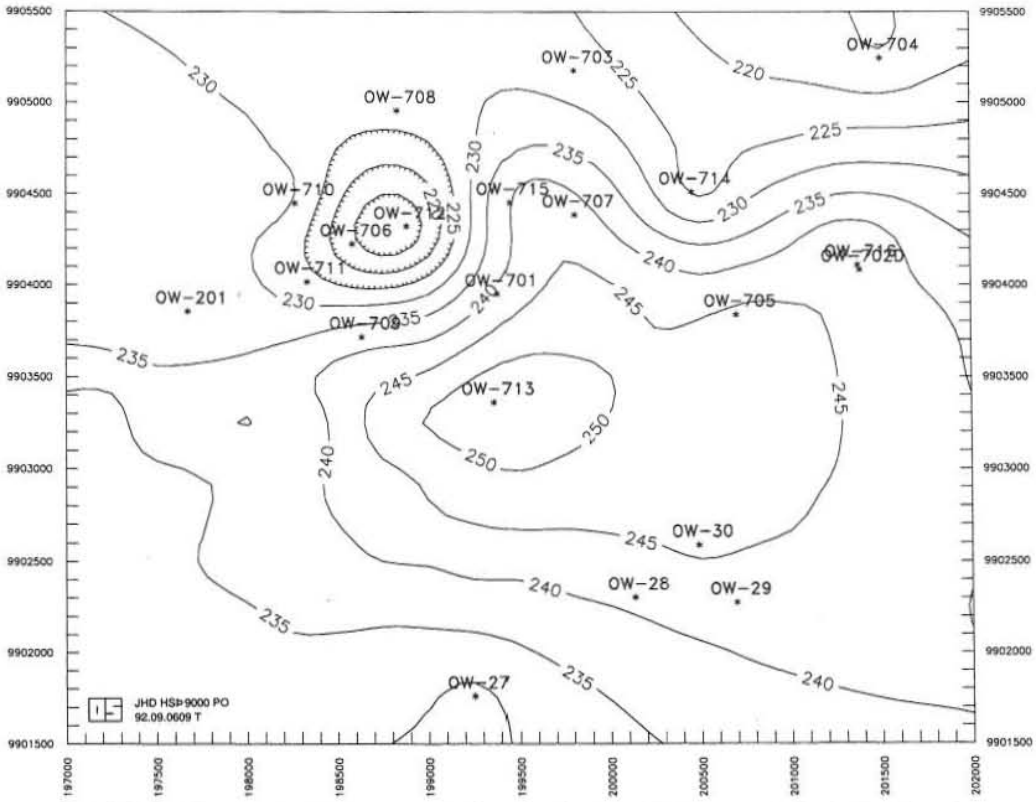

FIGURE 8: The temperature distribution at 500 m a.s.l. in NE-Olkaria

water on the fault which then flows laterally along the fault and north and south of it. Boiling occurs as the fluid rises forming a 240°C steam zone which is confined by caprock at 1300-1400 m a.s.l. as expressed in the temperature profiles. It can also be concluded from the temperature distribution that NE-Olkaria field is bounded in the west by the Ololbutot fracture zone, and in the north and northeast by the inferred arcuate fractures running close to wells OW-501 and 704. The E-Olkaria production field lies to the south.

The pressure potential in the field is generally such that stable water levels reach 1600-1700 m a.s.l. as indicated in Figures 9 and 10. Figures 11 and 12 show the planar pressure distribution in the field. The reservoir pressures are highest in the northeast close to the field boundary. This is probably indicating colder fluids encroaching upon the geothermal system. Within NE-Olkaria field pressures decrease southwards from 100 bara at 500 m a.s.l. in the Olkaria fault region to 86 bara at the southwestern border close to OW-709. This pressure distribution reflects the rising plume of boiling reservoir fluid in the NE-Olkaria field and subsequent southward flow of the boiling fluid.

2.3 Fluid Chemistry

Table 1 shows results obtained from geochemical analysis of water samples of fluids from selected wells in the NE-Olkaria field (Arusei, 1991; Merz and McLellan-Virkir, 1986). Water of the sodium-chloride type characterizes the deep reservoir. On the boundaries of the hot reservoir where mixing with cooler water occurs, sodium-bicarbonate type waters develop as can be seen in wells OW-201, 501 and 704. Sodium-bicarbonate type waters also develop above the geothermal reservoir due to condensation of steam in cooler water of perched aquifers.

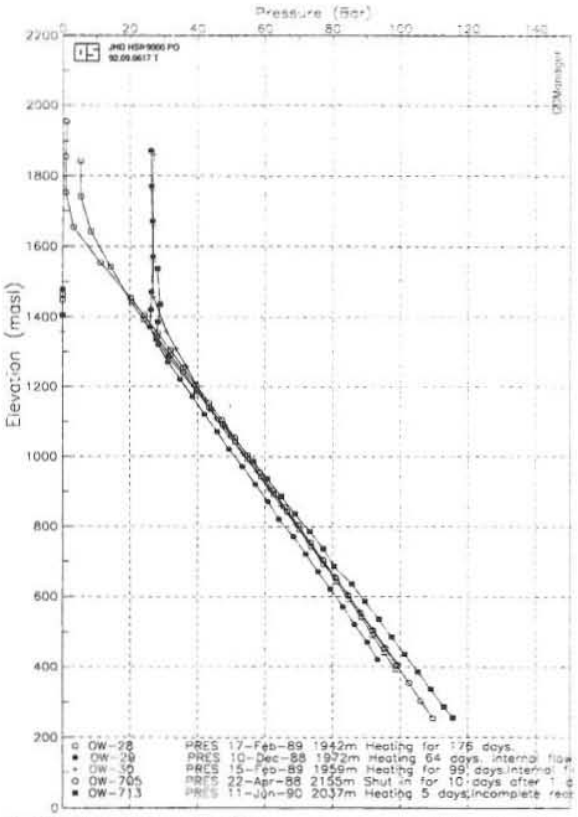

FIGURE 9: Stable pressure profiles in the south sector of NE-Olkaria

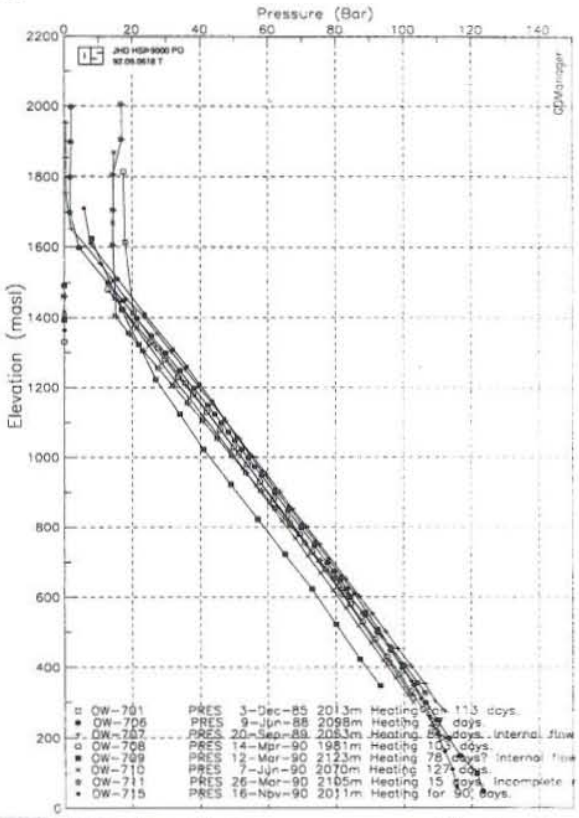

FIGURE 10: Stable pressure profiles in the north sector of NE-Olkaria

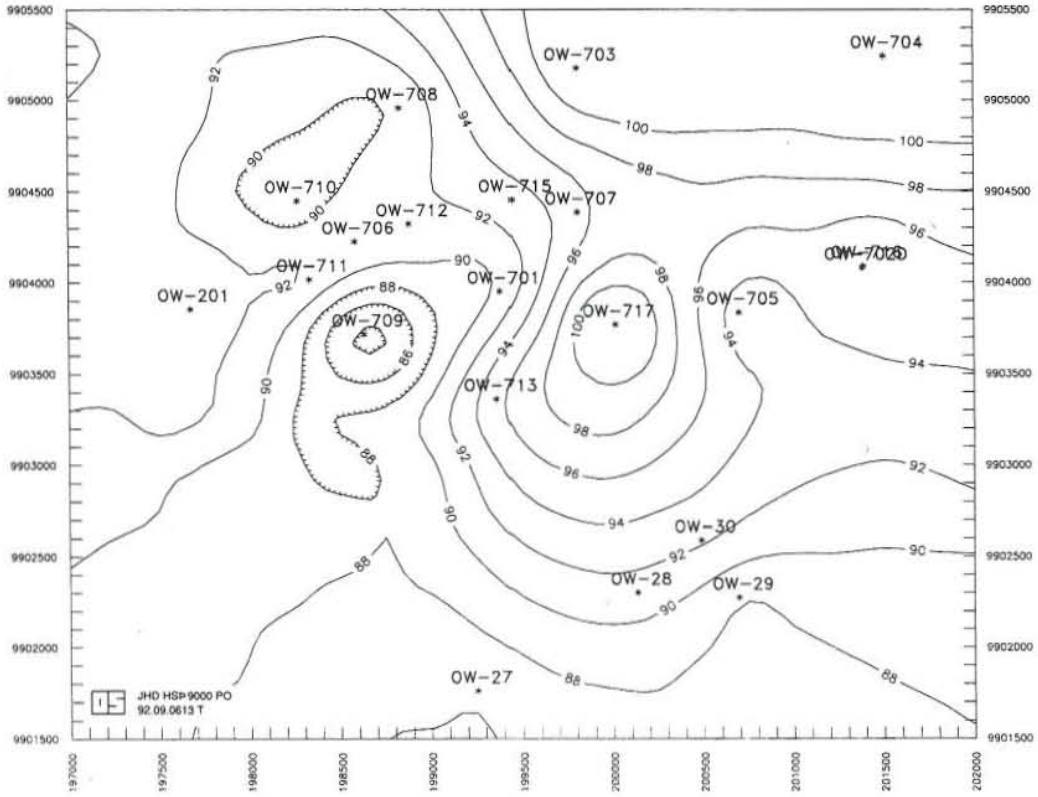

FIGURE 11: The pressure distribution at 500 m a.s.l. in NE-Olkaria

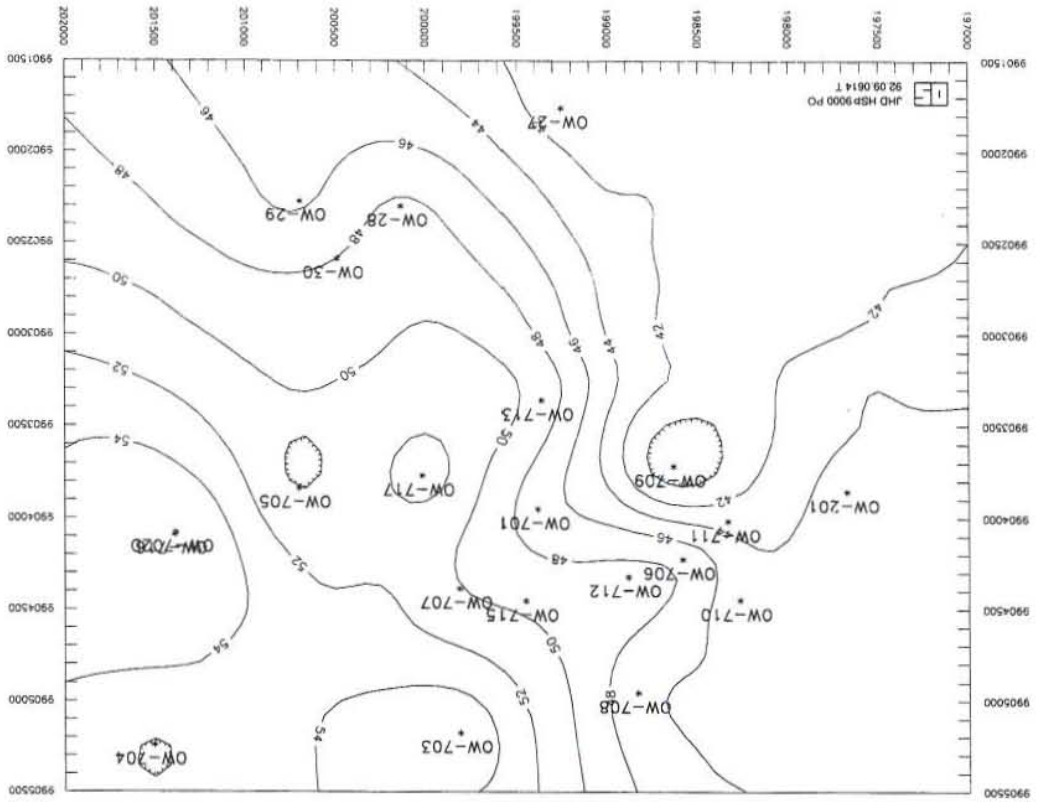

FIGURE 12: The pressure distribution at 1075 m a.s.l. in NE-Olkaria

TABLE 1: Chemical composition in ppm of discharge from selected NE-Olkaria wells (pH values were measured at either 20°C or ambient temperature)

Well No.	pH	SiO_2	Na	K	Li	Ca	Mg	CO_2	SO_4	H_2S	Cl	F	I *1000	Br *100	B	TDS
OW-701	9.6	713	511	90	4.6	0.47	Nil	176	?	9.5	634	?	-	-	0.96	2263
OW-714	9.7	522	570	106	1.6	Nil	Nil	169	68.4	2.69	635	58.7	174	159	3.2	2434
OW-715	9.0	576	576	94	1.56	Nil	Nil	140	28.4	1.02	601	33.0	174	174	3.2	2156
OW-716	8.0	624	624	124	2.34	Nil	Nil	60	82.5	0.26	899	38.0	240	174	6.2	2908
OW-201	9.3	394	1200	130	1.50	Nil	Nil	686	22.3	11.6	852	178	-	-	4.1	3414

The sodium-chloride type waters in Northeast Olkaria are relatively diluted and reducing and not corrosive. The steam quality is good, with about 0.3% total gas in the steam by volume (0.7% by weight) (Arnorsson et al, 1990). Calcite scaling downhole is not expected to be a problem. Provided that waste water is appropriately treated, silica deposition should not cause any operational difficulties in disposing of this water by reinjection.

2.4 Hydrology

The general pattern of groundwater movement is from the escarpment areas into the Rift Valley and southwards from Lake Naivasha area. Major inflow into the Olkaria geothermal reservoir is expected to be from the north and is probably concentrated along N-S striking faults and fractures. Inflow from other directions and from above is also possible because the pressure potential within the geothermal reservoir is lower than that of the surrounding groundwater and above lying perched aquifers.

2.5 Conceptual reservoir model

Figure 13 describes the present conceptual reservoir model of the NE-Olkaria field (Ewbank Preece-Virkir, 1989). The caprock for the system is basalt at a depth of 500 to 700 m and overlain by a lens of saline water. Fluid flow within the geothermal reservoir is dominated by convection. Two major upflow zones have been identified on either side of Olkaria Peak, both related to the Olkaria fault running WSW-ENE across the Olkaria field. Boiling fluids from those upflow zones flow laterally along the Olkaria fault and mix with colder water flowing southwards along a central zone bounded by the Olbutot fracture zone in the east and a parallel fracture zone in the west running through Olkaria Peak.

The upflow zone that has been inferred to exist to the north of the East Olkaria field causes a large southward pressure gradient. This causes significant lateral flow and results in a separation of vapour and liquid phases so that a steam zone of increasing thickness has been found in the southern part of the field. Underlying this steam is a boiling hot water reservoir that extends to depths of at least 2500 m where temperatures reach 340°C.

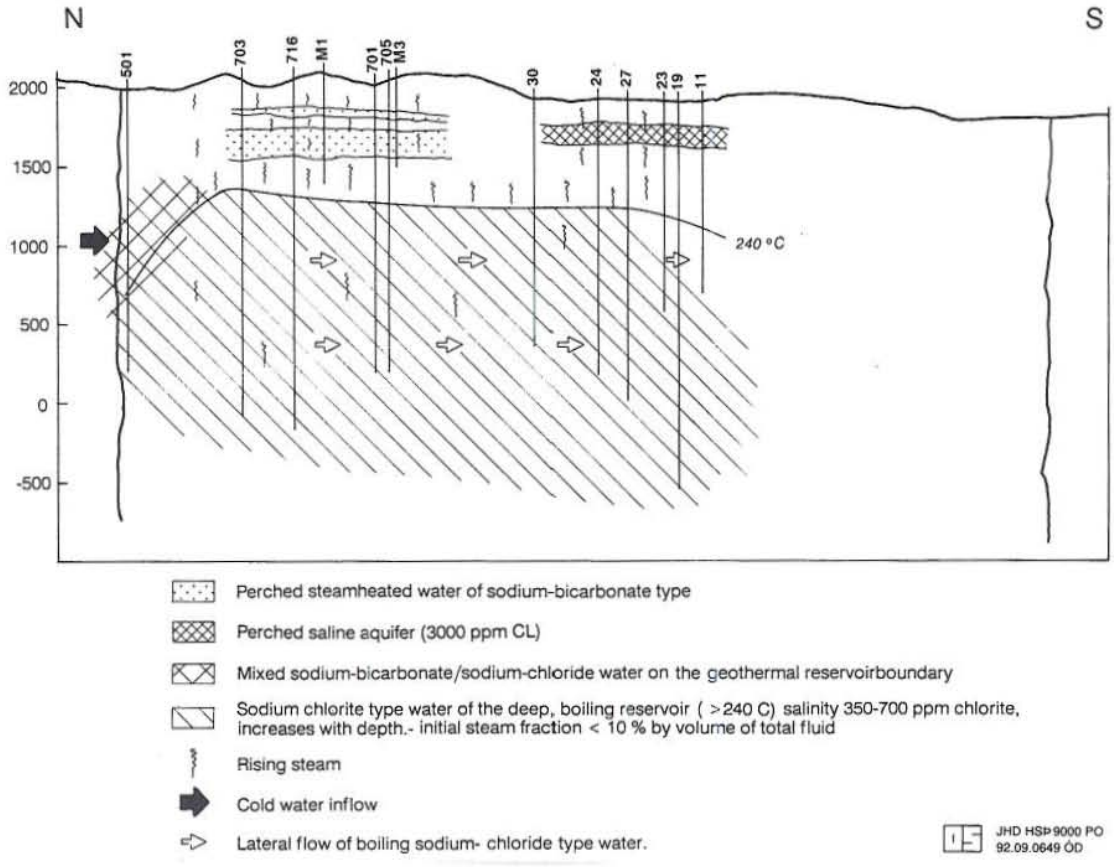

FIGURE 13: The present conceptual reservoir model of the NE-Olkaria geothermal system (Ewbank Preece - Virkir, 1989)

3. WELL CHARACTERISTICS

3.1 General

The well casing programme for NE-Olkaria wells consists of 20" diameter surface casing, 13 3/8" dia. anchor casing, 9 5/8" dia. production casing and 7" dia. slotted liners (Figure 14). The production casing depth usually extends to 1300-1600 m a.s.l (or 600-900 m depth) depending on the elevation of the wellhead. The total drilled depths of the wells range between 1800-2500 m. In the wells drilled during the latter part of the field appraisal, deeper production casing depth of ≥ 800 m and total drilled depth of ≥ 2200 m have been preferred. Table 2 gives an overview of the wells that have been drilled so far.

TABLE 2: An overview of NE-Olkaria wells

Well No.	Elevation (m)	Eastings	Northings	Tot.drilled depth (m)	Product. cas.depth (m)
OW-701	2012.9	199385.7	9903951	1803.5	620.3
OW-702D	2169.6	201384.4	9904080	1885.9	717
OW-703	2088.7	199810.2	9905176	2194.9	717
OW-704	2175.6	201504.4	9905244	2005.7	886
OW-705	2154.9	200701.7	9903836	2003.0	690
OW-706	2098.0	219585.2	9904224	2098.0	702
OW-707	2053.1	199811.0	9904386	1797.0	647
OW-708	1980.7	198833	9904956	1799.0	650
OW-709	2123.3	198635	9903717	1898.0	703
OW-710	2069.5	198269	9904449	1799.6	654
OW-711	2105.2	198333	9904017	1802.0	645
OW-712	2081.5	198885	9904321	2015.0	646
OW-713	2036.6	199364	9903361	1798.0	632
OW-714	2156.0	200458	9904510	2497.0	642
OW-715	2010.8	199451	9904454	2003.0	647
OW-716	2169.5	200757	9904719	2291.0	593
OW-717	2097.6	200012	9903751	2101.0	652
OW-718	2072.5	199830	9903543	1899.0	639
OW-719	2044.2	199646	9903813	2210.0	648
OW-720	2087.8	198956	9903778	2175.0	645
OW-721	2162.8	198758	9903381	2201.0	724
OW-722	2021.9	199338	9903658	2198.0	698
OW-723	2164.9	200581	9904178	2205.3	779
OW-724	2176.7	200816	9904398	2205.5	781
OW-725	2137.4	200240	9904295	2197.5	797
OW-726	2026.8	199818	9904094	2206.6	799
OW-727	2018.8	199226	9904187	2200.0	798

3.2 Lithology and aquifers

The wells display low permeability as observed from pressure transient tests. The transmissivity values range between 3-10 darcy-meters but average only 3.0 darcy-meters. Table 3 gives the summary of test results for the wells that will be considered for the design of the steam gathering system.

Most wells in this field develop wellhead pressure while shut-in but a few have to be compressed to initiate discharge. The wells discharge fluids with enthalpy ranging between 1100-2400 kJ/kg and total mass flowrate ranging between 9-65 kg/s at average wellhead pressure of 6 bara.

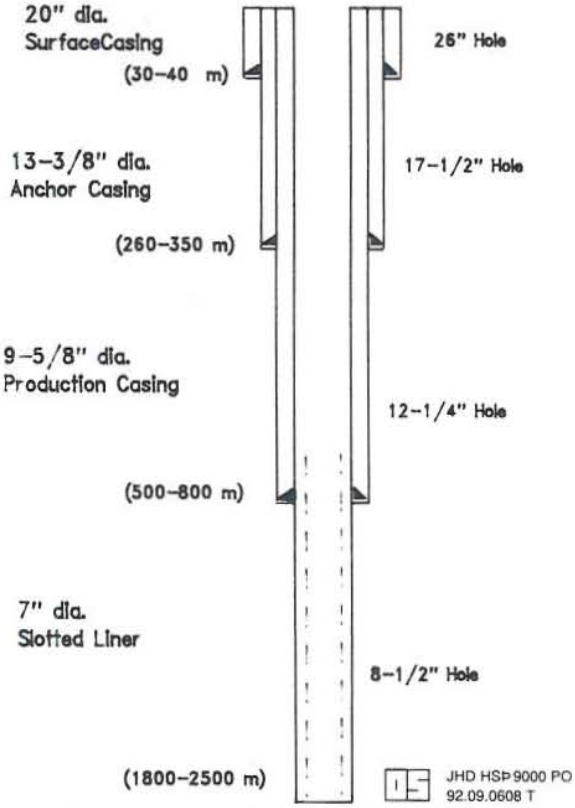

FIGURE 14: The casing programme for NE-Olkaria wells

Permeable horizons in wells occur at 1050-1400, 600-1000 and -50-200 m a.s.l. Aquifers at 1050-1400 m a.s.l. are at lower pressure potential and tend to be richer in steam than those at lower elevations. Cycling phenomenon has been observed in most wells during discharge. The fluctuations observed can be attributed to the variation in pressure potential among the aquifers feeding the wells combined with the random nature of the permeability distribution across these aquifers. Attempts have been made to set the production casing deeper than 1400 m a.s.l. in some wells in order to case off the aquifers at 1050-1400 m a.s.l. to try to eliminate fluctuations during discharge, with mixed results.

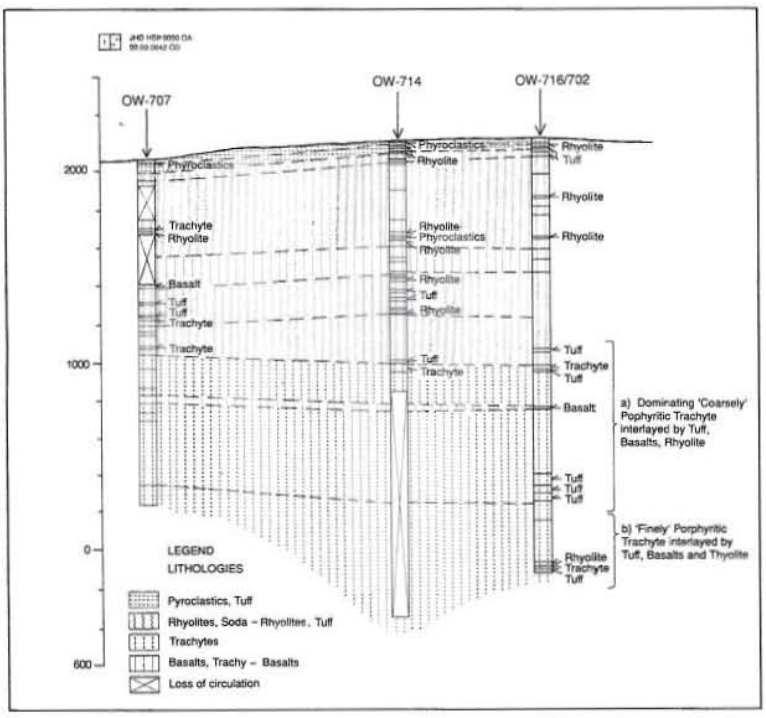

FIGURE 15: Geological correlation of NE-Olkaria wells

The reservoir rocks consist of successions of interfingering lavas of rhyolite, trachyte, and basalt with tuff intercalations. Although the successions appear to be near horizontal, individual units show considerable variations in thickness and distribution from well to well (Figure 15).

Aquifers seem to be related mostly to the layering of the volcanic pile or contraction fractures in lavas. The best producers within this part of Olkaria lie on a WSW-ENE trending zone consisting of wells

TABLE 3: Test results from selected wells in NE-Olkaria

Well No.	Feeder zones depth (m)	K h ($*10^{-12}$ m^3)	Enthalpy (kJ/kg)	Mass flow (kg/s)
OW-701	620-700 946-1000 1000-1200	10	1300	36
OW-705	850-950 1000-1300 below 1750	2.5	1500	18
OW-706	800-950 1050-1150 1350-1450 1550-1650	3.5	1650	23
OW-707	750-850 1250-1350	3.5	1250	25
OW-709	1400-1500 1800-bottom	10	2032	29
OW-710	650-850 1250-1450	2.4	1336	18
OW-711	650-900 1350-1700	2.3	1672	10
OW-712	1000-1200 1350-1500 2000-2020	2.3	2050	10
OW-713	700-1200 1550-1650	2.5	1731	9
OW-714	850-1100 1550-1650 1900-2200	2.4(?)	1377	65
OW-715	700-1100 1400-1800	2.7	1404	24
OW-716	800-1200 1900-2200	5.1	2386	14
OW-718	700-1400 1500-1700	6.9	1112	28
OW-719	800-1200 1800-2000	-	1295	42
OW-720	650-850 1100-1300 2000-2150	-	2236	9
OW-721	800-1100 1300-1600 1800-2100	1.8	1647	22
OW-725	850-1250 1600-1950 ~2000	3.3	1421	25
OW-726	800-1300 1800-2050 ~2200	3.6	1642	21
OW-727	850-1300 1800-2000 ~2100	3.0	1763	12

OW-709, 706, 701, 719, 715, 714 and 716 (see Table 3 and Figure 2). These wells are located relatively near the Olkaria fault suggesting that this fault represents an anomaly of enhanced permeability. Permeable horizons in Northeast Olkaria wells have been encountered in the depth range 650-2200 m. No correlation has been observed between lithology, permeability and depth.

3.3 Discharge/output characteristics

The discharge obtained from the wells is a two-phase mixture of steam and water. The technique used to quantify the discharge is the critical lip pressure method based on the following formula deduced by Russel James in 1970. The well is discharged through a lip pressure pipe into a silencer. The critical pressure at a lip pipe is measured together with the water flowrate from the silencer (Figure 16). The James formula is

$$m = 1{,}839{,}000 A \frac{P_c^{0.96}}{H^{1.102}} \qquad (1)$$

where

m = total mass flowrate, kg/s;
A = areal cross section of the lip pipe, m^2;
P_c = critical pressure at the end of the pipe, bara;
H = total fluid enthalpy, kJ/kg.

The flowrate can also be expressed in terms of water flowrate and total fluid enthalpy as follows:

$$m = W \frac{2274}{2666 - H} \qquad (2)$$

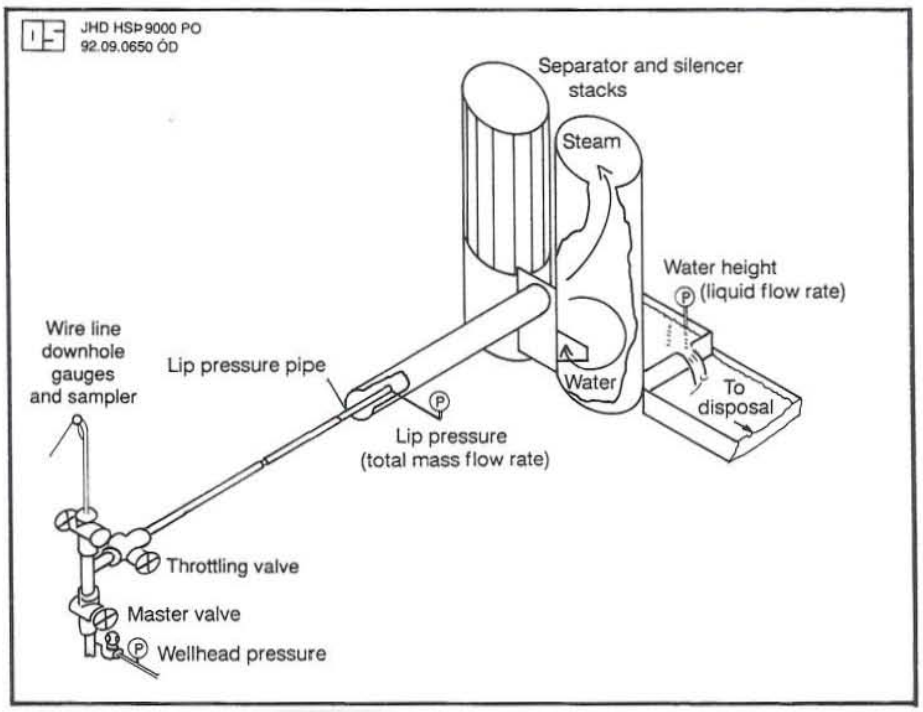

FIGURE 16: Equipment for output measurement using the lip pressure method.

where

W = water flowrate in kg/s after separation at atmospheric pressure, which is 0.8 bara at Olkaria.

Combining Equations 1 and 2 we obtain

$$\frac{W}{808.7AP^{0.96}} = \frac{2666 - H}{H^{1.102}} \qquad (3)$$

Readings of water level in the weir-box allows the water flowrate to be calculated and the water flowrate and critical lip pressure are substituted in Equation 3 in order to determine the total fluid enthalpy. The well output can then be calculated by Equation 1.

The discharge/output tests are carried out for periods lasting at least twelve (12) weeks. In order to construct output curves the well flowrates are varied using throttling valves. Due to the cyclicity observed during discharge tests of most wells, the discharge parameters taken for certain throttle conditions are averaged over a full cycle of discharge monitoring. Some of the wells exhibit such severe fluctuations during discharge that it may not be possible to use them to operate the power plant. If a cyclic well is to be connected to other wells in a gathering system then, whenever the discharge wellhead pressure becomes less than that in the rest of the system, backflow may occur. Therefore, if discharge tests establish that such conditions cannot be avoided in the discharge characteristics of a well by throttling or otherwise, then that well can be declared non-commercial. That is the criteria that has been used to select wells for the design of the gathering system (refer to Table 3). Output curves for the possible commercial wells in NE-Olkaria are contained in Appendix I.

4. PRELIMINARY DESIGN OF THE PIPELINE SYSTEM

4.1 The basis of the general lay-out of the system

Figure 17 shows a schematic diagram of the set-up proposed for Northeast Olkaria power plant. The wells to be connected to the power plant produce a two-phase mixture of vapour and water and are scattered over an area of about 6 km^2. The steam from these wells will be used to operate two 32 MW_e condensing turbine generators. The separated water will be reinjected back to the formation.

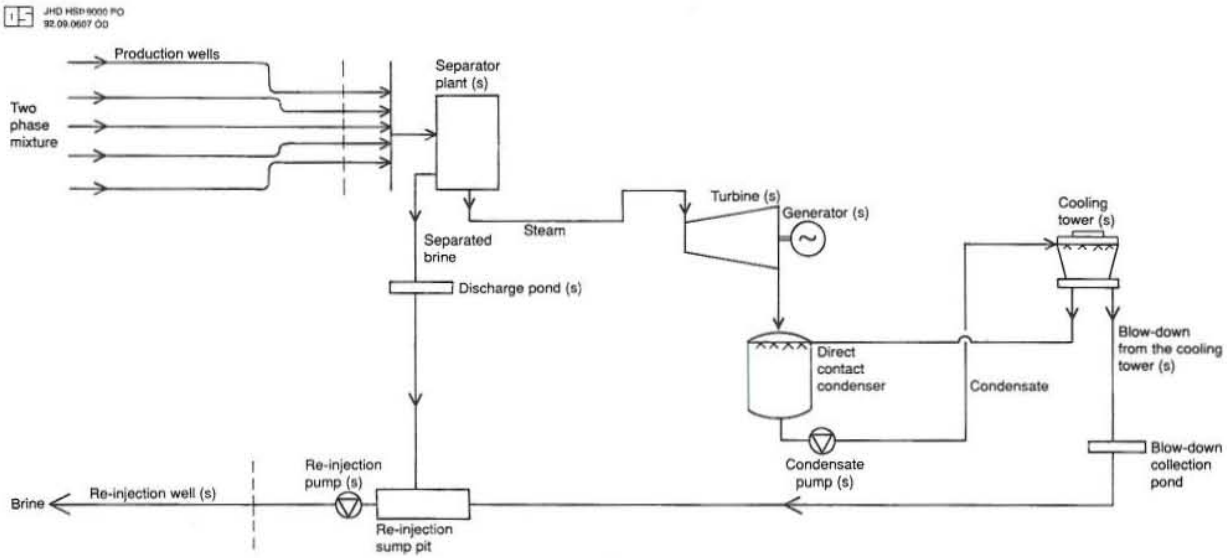

FIGURE 17: Schematic diagram of the set-up proposed for NE-Olkaria power plant

In order to effect the reinjection programme an arrangement has to be designed to gather the effluent at a suitable point before piping it to the reinjection well(s). In this way costs of separation and reinjection equipment could be minimized and the whole operation greatly simplified. A pressure drop in a steam line, after separation, results in a significantly greater loss in available energy for exploitation through a turbine than a similar pressure loss in a two-phase line before separation. This is because although a pressure loss in a two-phase line reduces the available enthalpy drop of the steam component of the flow, in the same manner as for a pure steam line, the pressure drop also results in production of additional steam due to flashing of the water phase. There is no need to install steam traps, with their associated drains, on two-phase pipelines. Such a set-up could prove useful when considering a case of a double-flash system.

However there are two important disadvantages of the two-phase flow/central separation. The flow from all wells is combined before separation and hence it is not possible to separately measure the discharge from individual wells unless it is isolated from the station supply and discharged to atmosphere. The two-phase pipelines must generally be designed to maintain moderately high steam velocities so that two-phase flow occurs in the stable annular flow regime. As a consequence of the moderately high steam flow velocity and also the additional friction due to the different water and steam velocities in the pipe, the pressure drop in a two-phase pipeline is generally several times greater than the typical pressure drop for the steam pipework.

A drawing of the proposed Northeast Olkaria steamfield arrangement is shown in Figure 18. When considering the geographical distribution of Northeast Olkaria resource area it is apparent

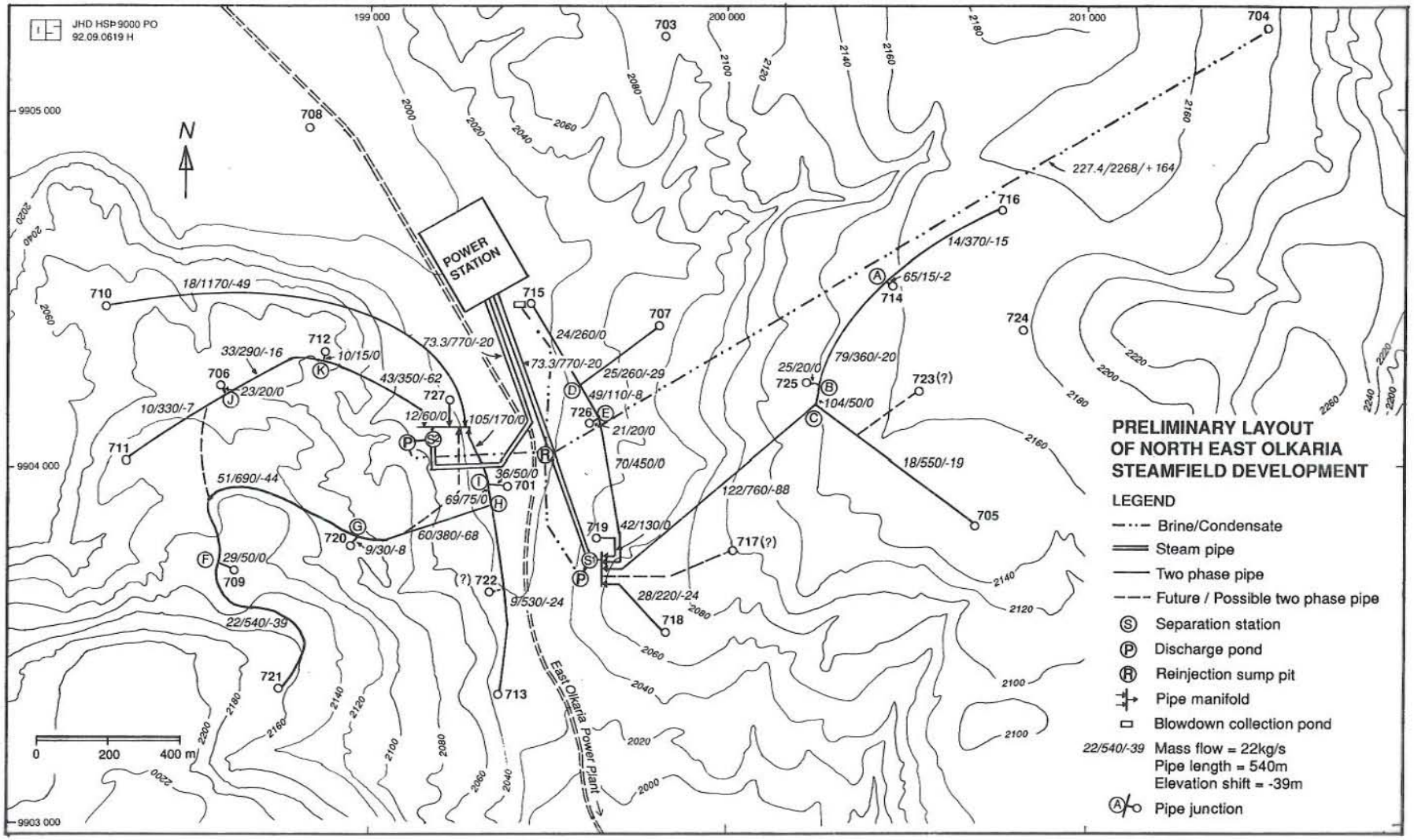

FIGURE 18: The proposed layout for the NE-Olkaria steamfield arrangement

that in the vicinity of the proposed power station site (beside the main road north of OW-M1), the field is reasonably uniformly spaced on each side of the main road. The well field is divided into eastern and western sectors by the main road crossing the field. This fact naturally leads to the concept of having the wells to the eastern side connected by two-phase pipelines to separation station S1 and similarly wells to the western side to separator station S2. The steam obtained will be transmitted by pipework to the power station with each separator station providing the steam for one of the two 32 MW_e units. The separated water will be flashed to atmosphere with the residual hot water being conveyed by open drains to a reinjection sump pit from where it will be pumped to the reinjection well(s).

This concept has the advantage of minimizing the amount of pipework that needs to cross the main road, limiting this to only the steam and reinjection pipelines/open drains from the western separation station. There is a further advantage in avoiding the need for two-phase lines to cross the road in that a drop loop would be required through a road culvert which would present an undesirable opportunity for water accumulation.

4.2 Pipeline lay-out

It is desirable to arrange a downhill flow direction of the two-phase pipework from the wells to the separation station where possible. This ensures that water cannot accumulate in the pipework and also minimizes the pressure drop along the pipeline by achieving an advantage from the head of the two-phase fluid. The pipeline routes have been placed near roads whenever possible. Expansion is to be allowed for in the layout, preferably utilizing expansion loops rather than expansion bellows.

Consequently, the separation stations have been located downhill from the production wells. It has, therefore, been proposed to locate them on the low flat areas on each side of the main road in the vicinity of well OW-701. It has also been proposed to construct a separate sump pit for the reinjection pumps which would be located beside the main road as shown in Figure 18. In this location the waste water from each separation station discharge pond would be able to flow to the reinjection sump pit using only gravity head from a decanting overflow inlet at each pond.

The distance that the separator stations have been positioned from the power station has been determined by steam scrubbing considerations. Although separation efficiencies of 99.9 % (mass) water or better would be expected from the cyclone separators, a very small quantity of water droplets will, nevertheless, be carried over with the steam phase into the steam transmission pipeline to the turbines. Deliberately designing the steam pipeline to allow some condensation to occur provides a very important diluting and scrubbing effect on the carried-over droplets of geothermal water. These droplets will contain salts and also potential scaling compounds which, if not removed, can lead to stress corrosion cracking and the build-up of scale in the turbine. The condensate can be drained through drainpots which would be located at intervals along the main steam transmission line.

4.3 Two-phase flow pressure drop calculation methods

The pressure drop (Δp) is a parameter of great importance in the design of systems with phase change. In forced-circulation systems the pressure drop governs the pumping requirements. In gravitational flow the pressure drop dictates the flowrate and, hence, the other system parameters.

A large number of models and correlations are available for predicting two-phase flow pressure drop. Basically it is possible to distinguish three fundamental physical models. The **homegenous** flow model is the simplest. This assumes that the liquid and the gas or vapour are uniformly distributed over the flow cross-section and in the flow direction so that the mixture can be regarded as single phase with suitably defined mean values of the thermodynamic and hydrodynamic properties of the two phases.

In the **separated** flow model, or **slip** model, it is assumed that the gas and the liquid flow separately as continuous phases with distinct mean velocities within different parts of the flow cross-section. A set basic equation is formulated for each phase, and the solution is closed by expressions detailing the interaction of the two phases and the interaction of the two phases with the channel walls. These are obtained from emperical equations which give the mean void fraction, defined as the mean proportion of a pipe cross-sectional area containing the gaseous phase, or the ratio of the mean velocities (slip) and the wall shear stress as a function of the primary parameters of flow.

None of the general correlations for predicting the pressure drop is particularly accurate. This is partly due to their failure to explicitly include factors, such as entrance conditions, that are important and whose influence can persist for hundreds of diameters downstream of the entrance. The inaccuracy is also due partly to the fact that the same correlation is used to represent many different physical situations; that is, in general correlations, no particular reference is made to flow pattern, and this has a profound effect on fluid-fluid interaction, and hence on pressure drop.

More realistic representations of two-phase flow have recently appeared in the literature as the third type of two-phase models. These models involve treating various phase models independently, e.g annular model, slug model, etc. The description of any flow pattern is generally accomplished by means of statistical features of the flow or by means of mass, force and energy balances. However, the analysis is difficult. Only the relatively simple annular and stratified flows have been analysed in this way (Freeston, 1982).

4.3.1 Basic equations

In developing the equations, use has been made of the basic conservation laws for mass, momentum and energy. The following assumptions have been made:

1. At any one cross-section of the channel, the fluid pressure is constant.
2. The velocity of a phase (liquid or gas) is essentially constant across the channel, although there may be a difference between the velocities of the phases.

During two-phase flow in a non-horizontal channel the pressure drop per unit length is made up of contributions due to friction, acceleration and elevation (gravity), i.e.:

$$\frac{dp}{dz} = \left(\frac{dp}{dz}\right)_f + \left(\frac{dp}{dz}\right)_a + \left(\frac{dp}{dz}\right)_g \qquad (4)$$

The equation of the individual components can be defined by means of momentum balance. Substituting for terms on the right hand side of Equation 4 it can be rewritten as (Hewitt, 1982) where

$$\frac{dp}{dz} = \frac{\tau_o P}{A} + m^2 \frac{d}{dz}\left[\frac{(1-x)^2}{\rho_L(1-\alpha)} + \frac{x^2}{\rho_G \alpha}\right] + g\rho_{TP}\sin\theta \qquad (5)$$

τ = wall shear stress;
P = channel periphery;
A = channel cross-sectional area;
m = mass flowrate;
x = steam fraction;
α = void fraction;
ρ_L = liquid density;
ρ_G = vapour density;
ρ_{TP} = two-phase density;
θ = angle between the pipe axis and the horizontal;
g = gravitational acceleration.

The last two terms in Equations 4 and 5 describe a reversible change of pressure; the frictional pressure drop, however, is an irreversible change of pressure resulting from energy dissipated in the flow by friction, eddying, etc.

The definition of the two-phase density (mean density of the two phases) is dependent upon the model chosen (Freeston, 1982). For homogeneous flow it is

$$\frac{1}{\rho_{TP}} = \frac{x}{\rho_G} + \frac{1-x}{\rho_L} \qquad (6)$$

and for the separated flow model

$$\rho_{TP} = \alpha\rho_G + (1-\alpha)\rho_L \qquad (7)$$

and a correlation for α (void fraction) is necessary.

During the flow of two-phase mixture through a pipe there is an increase in volumetric flow due to reduction in pressure caused by friction and, in a single component mixture, due to flashing. This results in an increase in the velocity of both phases with a resultant momentum change, giving a pressure drop due to acceleration. In order to estimate this we need first to estimate the void fraction.

For the typical pressure range used in geothermal pipelines, 5 to 12 bar, Harrison modified the correlation by Butterworth (Freeston, 1982) using the data from the NZ MWD file to obtain Equation 8

$$\alpha = \frac{1}{1 + \left(\frac{1-x}{x}\right)^{0.8}\left(\frac{\rho_G}{\rho_L}\right)^{0.515}} \qquad (8)$$

This correlation neglects the possible effects of a) flow regime, b) inclination of channel and c) high mass transfer rates. But this is the one that will be used as, in practical cases, the acceleration term is small.

In general the friction term contributes most to the overall pressure drop; however its calculation is imprecise with the result that many pipes and flow channels are over or undersized. Often the frictional pressure drop in two-phase flow is referred to as that of a single-phase flowing under certain hydrothermal conditions. This relating factor is called the " Two-Phase Multiplier" . It can relate the two-phase frictional pressure gradient to that for the gas or liquid phase flowing alone in the pipe, in terms of frictional multipliers ϕ_G and ϕ_L defined as follows:

$$\phi_G^2 = \frac{(dp/dz)_{fTP}}{(dp/dz)_{fG}} \tag{9}$$

$$\phi_L^2 = \frac{(dp/dz)_{fTP}}{(dp/dz)_{fL}} \tag{10}$$

where $(dp/dz)_{fTP}$ is the two-phase pressure gradient and $(dp/dz)_{fL}$ and $(dp/dz)_{fG}$ are the pressure gradients for the liquid phase and the steam phase flowing alone in the pipe. It is convenient to relate the two-phase frictional pressure gradient to that for the steam phase flowing alone in the pipe, in terms of a frictional multiplier as already defined. Therefore, in the discussion to follow, the two-phase frictional pressure gradient will be related to that for the steam phase.

The literature contains numerous relationships and calculation models for the multiplier. One of the favoured methods using the friction multiplier approach is the Lockhart-Martinelli correlation (Hewitt, 1982). This correlation has its limitations; it does not contain surface tension as a parameter and fails to take adequate account of the influence of mass flux. The Lockhart-Martinelli correlation tends to overpredict the pressure drop as reported by Harrison (Freeston, 1982). In order to obtain the multiplier we define the pressure drop ratio or (Lockhart-Martinelli parameter)^2 as

$$X^2 = \frac{(dp/dz)_{fL}}{(dp/dz)_{fG}} = \left(\frac{1-x}{x}\right)^{1.8}\left(\frac{\rho_G}{\rho_L}\right)\left(\frac{\mu_L}{\mu_G}\right)^{0.2} \tag{11}$$

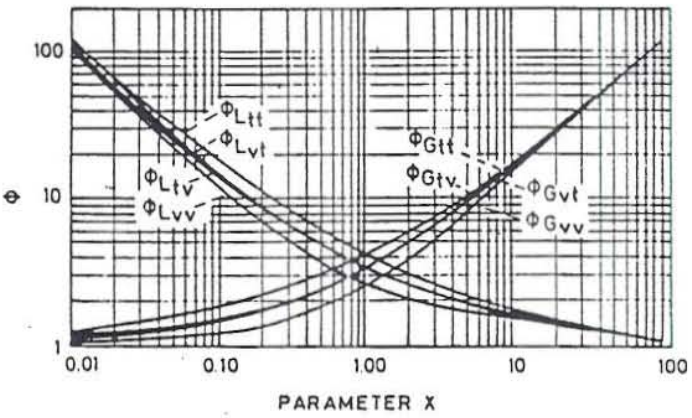

FIGURE 19: The correlation of Lockhart and Martinelli for two-phase multipliers

Lockhart and Martinelli presented the relationship between the two-phase multiplier, ϕ, and the pressure drop ratio, X, in graphic form, as illustrated in Figure 19. Different curves were suggested, depending on whether the two-phase-alone flows were laminar ("viscous") or turbulent, and the multipliers are subscribed accordingly. For example, the multiplier ϕ_{Gtt} applies to the case in which both the steam and liquid phases flowing alone in the pipe are turbulent. Curve fit of this graph gives the two-phase multiplier as

$$\phi_G^2 = e^{3.039X^{0.38}} \tag{12}$$

which is valid for $X < 1$ and annular or stratified flow (Jonsson, written com.).

The single-phase pressure drop for steam can be calculated from the standard equation

$$(\frac{dp}{dz})_G = f\frac{L}{D}\frac{1}{2}\rho_G V_G^2 \tag{13}$$

Consequently the two-phase flow pressure drop equation becomes

$$\Delta P = (\frac{dp}{dz})_{f_{TP}} = \phi^2 f\frac{L}{D}\frac{1}{2}\rho_G V_G^2 \tag{14}$$

where

ΔP = two-phase pressure drop, N/m^2;
ϕ^2 = two-phase multiplier, dimensionless;
f = friction coefficient;
L = effective length, m;
D = inside diameter of pipe, m;
ρ_G = density of the steam, kg/m^3;
V_G = velocity of steam if it was flowing alone in the pipe, m/s.

The velocity of steam can be expressed as

$$V_G = \frac{4mx}{\rho_G \pi D^2} \tag{15}$$

The two-phase pressure drop due to friction then becomes

$$\Delta P = \frac{8}{\pi^2}\phi^2\frac{Lf}{D^5}\frac{(mx)}{\rho_G} \tag{16}$$

The friction coefficient, f, is a function of Reynolds number, R_e, and pipe wall roughness, ϵ. The Reynolds number for the steam phase is

$$R_{e_G} = \frac{\rho_G V_G D}{\mu_G} \tag{17}$$

where

μ_G = dynamic viscosity for the steam phase, kg/ms.

For rough pipes the following correlation for f by Colebrook and White is widely used

$$\frac{1}{\sqrt{f}} = 1.74 - 2\log(\frac{2\epsilon}{D} + \frac{18.7}{R_e\sqrt{f}}) \tag{18}$$

For $R_e > 4*10^4$ Equation 18 can be approximated with (Jonsson, written com.)

$$f = \frac{1}{[2\log(\frac{0.27\epsilon}{D} + \frac{7}{R_e^{0.9}})]^2} \tag{19}$$

Friedel compared a data bank of 25,000 data points with existing correlations and with a new correlation that he developed (Hewitt, 1982). He found it convenient to relate the two-phase frictional pressure gradient to the frictional pressure gradient for a single-phase flow at the same total mass velocity and with the physical properties of the liquid phase, namely , $(dp/dz)_{fLO}$. The two-phase frictional multiplier in this case is defined by

$$\phi_{LO}^2 = \frac{(dp/dz)_{f_{TP}}}{(dp/dz)_{f_{LO}}} \tag{20}$$

and Friedel's correlation is

$$\phi_{LO}^2 = E + \frac{3.24FH}{Fr^{0.045}We^{0.035}} \tag{21}$$

where

$$E = (1-x)^2 + x^2\frac{\rho_L f_{GO}}{\rho_G f_{LO}}; \qquad F = x^{0.78}(1-x)^{0.24};$$

$$H = (\frac{\rho_L}{\rho_G})^{0.91}(\frac{\mu_G}{\mu_L})^{0.19}(1-\frac{\mu_G}{\mu_L})^{0.7};$$

$$Fr = \frac{m^2}{gD\rho_{TP}^2}; \qquad We = \frac{m^2 D}{\rho_{TP}\sigma}.$$

μ_L is the dynamic viscosity for liquid in kg/ms; σ is the surface tension in N/m, and f_{GO} and f_{LO} are the friction factors for the total mass flux flowing with steam and liquid properties, respectively.

For this particular correlation, ρ_{TP} is given by

$$\rho_{TP} = \left[\frac{x}{\rho_G} + \frac{1-x}{\rho_L}\right]^{-1} \tag{22}$$

The correlation given by Equation 21 is for vertical upward flow and horizontal flow. A slightly different correlation is used for vertical downflow.

Recent evaluations (based on Heat Transfer and Fluid Flow Service proprietary data bank) have led to the following tentative recommendations with respect to the published correlations (Hewitt, 1982):

1. For μ_L/μ_G < 1000, the Friedel correlation should be used.
2. For μ_L/μ_G > 1000 and m > 100, the Chisholm correlation (Hewitt, 1982) should be used.
3. For μ_L/μ_L > 1000 and for m < 100, the Martinelli correlation (Hewitt, 1982) should be used.

Based on the above recommendations, and for the range that we are working in, the correlation by Friedel should give the best results.

4.3.2 Losses at fittings

The equivalent length procedure has been adopted to present the pressure losses recorded at fittings. An estimate of 15% additional length has been added to the actual length of pipe in order to compensate for pressure losses in fittings (recommendation of VGK Consulting Engineers, Iceland, who have long experience in designing steam transmission pipelines). In this way the effective pipe length in Equation 16 has been calculated.

4.3.3 Flow pattern map

The usual way of presenting results of observations of flow patterns is to plot them on a graph whose axes represent the flowrates of the two phases. When all the observations have been recorded in an appropriate manner, lines are drawn on the graph to represent the boundaries between the various regimes of flow. The resultant diagram is called a "flow pattern map" or a "flow regime map". For horizontal flow, which is the one of interest to us, the best known and most widely used flow regime map is that of Baker (Hewitt, 1982), shown in Figure 20.

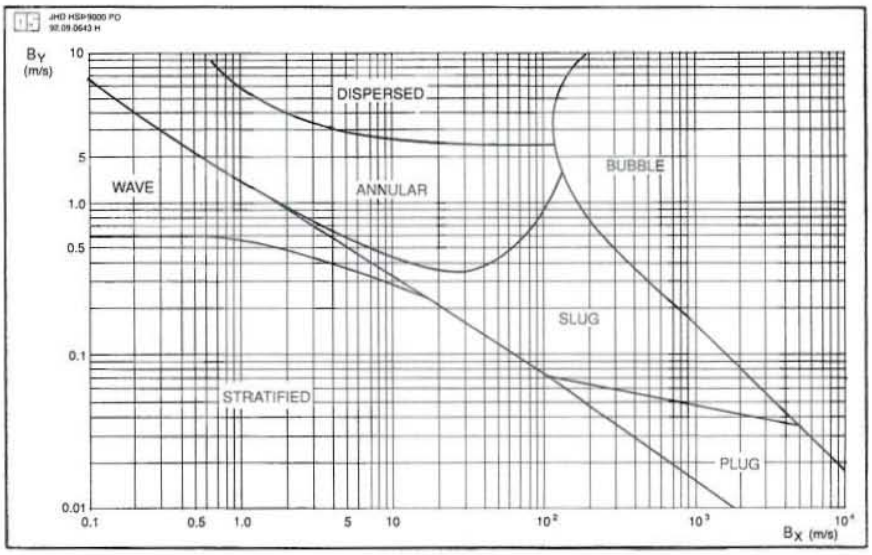

FIGURE 20: The Baker flow pattern map

The co-ordinates of the Baker chart are

$$B_x = 2.105\left(\frac{1-x}{x}\right)\left(\frac{\rho_G^{0.5}}{\rho_L^{0.166}}\right)\left(\frac{\mu_L^{1/3}}{\sigma}\right) \qquad (23)$$

and

$$B_y = \frac{2.752mx}{D^2\sqrt{\rho_L \rho_G}} \tag{24}$$

After every calculation of the total two-phase pressure drop and the superficial steam velocity V_G the Baker parameters, B_x and B_y, have been used to check the flow regime. In designing the two-phase pipelines, annular flow regime is preferred and slug regime avoided as much as possible.

4.4 Sizing and cost of pipelines

The sizing of the pipes was based on Pressure Class 16 PN and therefore the cost of steel has been done as per weight per unit length as specified in the standards. The pressure class used has been selected qualitatively by comparing with pressure class used in the design of steam gathering system in Svartsengi geothermal field in Iceland. The operational pressures in Svartsengi geothermal field are similar to those expected for NE-Olkaria geothermal field.

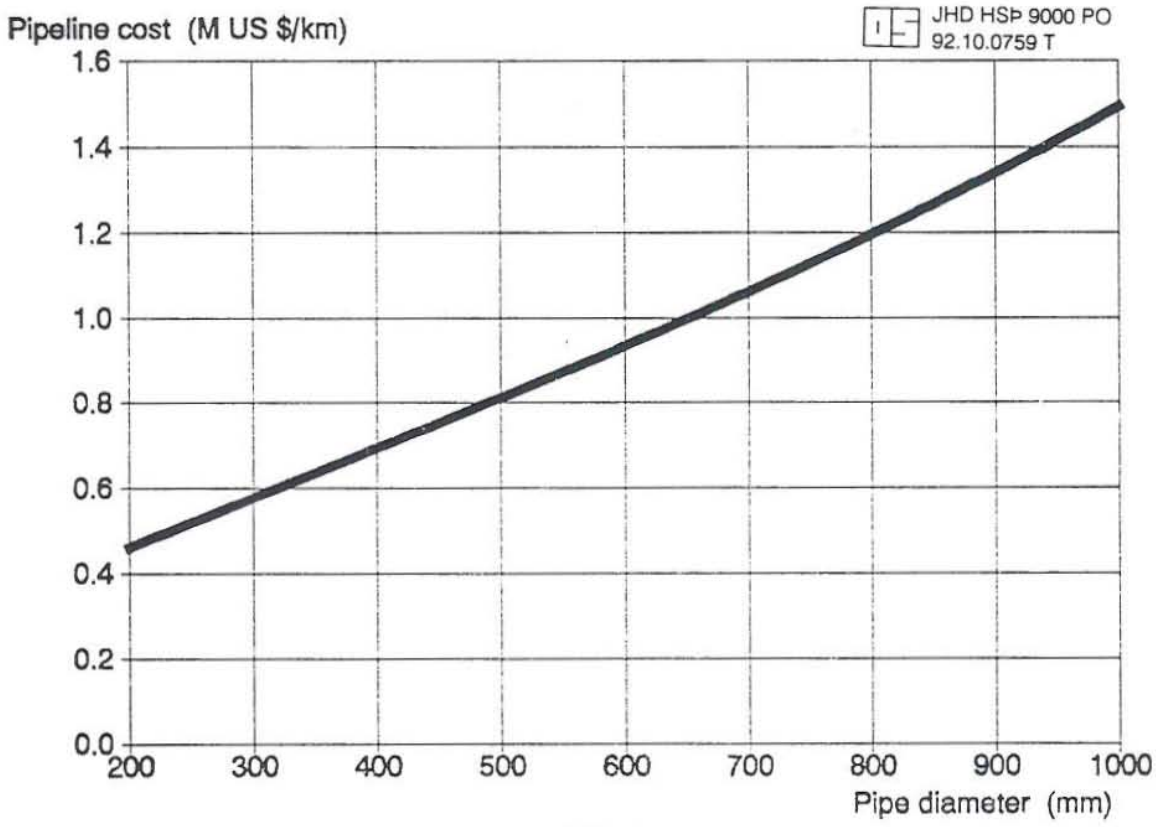

FIGURE 21: Total cost of steam pipelines as a function of pipe diameter

The cost estimates for the pipelines are based on a recent study carried out at Orkustofnun. The main results of this study are given in Figure 21 which shows the total cost of steam pipelines as a function of pipe diameter. The important parameters influencing the investment costs associated with costructing a geothermal steam transmission pipeline comprise material costs, construction costs, associated civil works, right of way of fees etc. The total capital cost is classified into pipe material costs, foundation costs, insulation costs, alluminium sheathing and civil work costs (such

as road works, landscaping etc.) and the relativity of these incremental cost classes depicted in the form of a bar chart (Figure 22, example for 500 mm diameter pipeline).

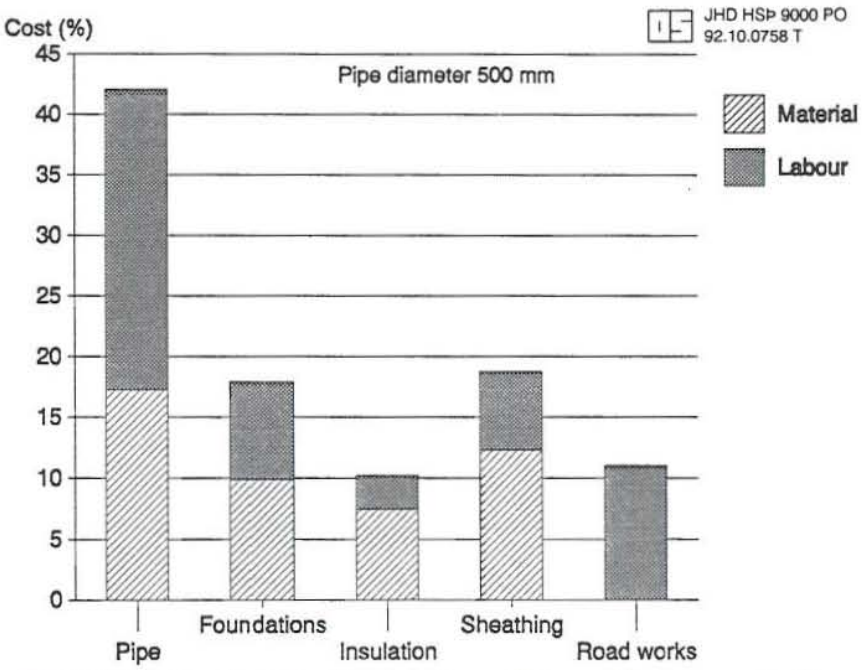

FIGURE 22: Cost distribution for a 500 mm dia. steam pipeline

In sizing the two-phase pipelines two different correlations for pressure drop have been used. One of them was developed by Lockhart-Martinelli and the other by Friedel (Hewitt, 1982). The Lockhart-Martinelli correlation has been applied in the form of a spread sheet whereas the Friedel correlation was applied in the form of a computer programme known as PIPE, developed at Orkustofnun. The computer printouts are listed in Appendix II showing results obtained, for pipeline S1-710, from both the spread sheet and the computer programme, PIPE.

Two-phase pipelines

The sizing of the two-phase pipelines has been based on allowable pressure drop between the well to the separation station with respect to the well output curve, superficial velocity of steam, V_G, and two-phase flow pattern. The criteria used is superficial steam velocity between 20-40 m/s and annular flow regime. The costs have been based on Figure 21.

Steamlines

A pressure drop of 0.1 bar has been allowed between the separation stations and the power plant in sizing the steamlines. The cost has also been based on Figure 21.

Reinjection pipelines

As for the costing of the reinjection pipelines the velocity of water has been restricted to between 1-2 m/s. The costs have also been based on Figure 21 except that insulation costs have been excluded.

4.5 Results

Table 4 summarizes the two-phase pipeline sizing, the expected operational wellhead pressure and the costs for such a network. The pressure values in the table are obtained by applying the Friedel

correlation for two-phase pressure drop. This correlation is considered to be more reliable in this case than the Lockhart-Martinelli correlation which overpredicts the pressure drop by 25-30%. Table 5 gives similar results as for Table 4 with some pipe sizes having been reduced to the immediate lower standard pipe diameter. It can be observed that some of the operational wellhead pressures have been raised to over 8 bara and the total costs lowered by 10% from 6.9418 M to 6.2554 M USD. Although the costs in Table 5 are lower as compared to those in Table 4 the operational wellhead pressures are not desirable for NE-Olkaria; hence the network summarized in Table 4 is the one proposed for the two-phase pipelines.

TABLE 4: Summary of two-phase pipeline sizing and costs

Line id.	Mass flow (kg/s)	Pipe length (m)	Elev. shift (m)	Tot. enth. (kJ/kg)	Norm. bore (m)	P_{OUT} (bara)	P_{IN} (bara)	Vap. vel. (m/s)	Pres. drop (bar)	Whp (bara)	Cost Thousands US$
S1-C	122	760	-88	1520	0.9	6.00	6.27	26.8	0.27		1021.4
C-705	18	550	-19	1500	0.4	6.27	6.63	19.4	0.36	6.63	381.2
C-B	104	50	0	1523	0.8	6.27	6.30	27.8	0.03		60.8
B-725	25	20	0	1421	0.4	6.30	6.32	24.5	0.02	6.32	13.9
B-A	79	360	-20	1556	0.7	6.30	6.53	28.5	0.23		381.6
A-714	65	15	-2	1377	0.5	6.53	6.56	36.5	0.03	6.56	12.1
A-716	14	370	-15	2386	0.4	6.53	6.87	28.4	0.34	6.87	256.4
S1-718	28	220	-24	1112	0.3	6.00	6.56	28.7	0.56	6.56	127.8
S1-719	42	130	0	1295	0.4	6.00	6.34	36.7	0.34	6.34	90.1
S1-E	70	450	0	1420	0.6	6.00	6.46	31.3	0.46		423
E-726	21	20	0	1642	0.35	6.46	6.50	33.5	0.04	6.46	12.7
E-D	49	110	0	1325	0.5	6.46	6.58	26.0	0.12		88.8
D-707	25	260	-29	1250	0.35	6.58	6.98	24.4	0.40	6.98	165.6
D-715	24	260	0	1404	0.35	6.58	7.08	29.0	0.50	7.08	165.6
S2-I	105	170	0	1692	0.9	6.00	6.07	27.3	0.07		228.5
I-701	36	50	0	1300	0.4	6.07	6.17	31.3	0.10	6.17	34.7
I-H	69	75	0	1897	0.7	6.07	6.13	34.9	0.06		79.5
H-713	9	530	-24	1731	0.25	6.13	7.05	27.9	0.92	7.05	275.6
H-G	60	380	-68	1921	0.7	6.13	6.33	30.6	0.20		402.8
G-720	9	30	-8	2236	0.3	6.33	6.36	27.5	0.03	6.36	17.4
G-F	51	690	-44	1866	0.7	6.33	6.59	24.1	0.26		731.4
F-709	29	50	0	2032	0.5	6.59	6.63	29.6	0.04	6.63	40.4
F-721	22	540	-39	1647	0.4	6.59	7.16	26.1	0.57	7.16	374.2
S2-727	12	60	0	1763	0.3	6.00	6.09	27.6	0.09	6.09	34.9
S2-K	43	350	-62	1748	0.6	6.00	6.18	26.7	0.18		329.0
K-712	10	15	0	2050	0.3	6.18	6.20	27.8	0.02	6.20	8.7
K-J	33	290	-16	1657	0.5	6.18	6.41	26.6	0.23		234
J-706	23	20	0	1650	0.35	6.41	6.46	37.3	0.05	6.46	12.7
J-711	10	330	-7	1672	0.3	6.41	6.69	19.9	0.28	6.69	191.7
S2-710	18	1170	-49	1336	0.35	6.00	7.20	22.0	1.20	7.20	745.3
Total length		**8325**	**Total cost of two-phase pipelines**								**6941.8**

Two steamlines, each of length 770 m and coming from separation stations S1 and S2, will transmit the separated steam to the power plant. These pipelines should be of 1000 mm nominal bore (Pressure Class 16 PN). The cost of these two steamlines will be = 2.2715 M USD.

The cost of the reinjection pipeline, 2266 m and 400 mm diameter, = 1.0992 M USD.

TABLE 5: Summary of two-phase pipeline sizing and costs (alternative network)

Line id.	Mass flow (kg/s)	Pipe length (m)	Elev. shift (m)	Tot. enth. (kJ/kg)	Norm. bore (m)	P_{OUT} (bara)	P_{IN} (bara)	Vap. vel. (m/s)	Pres. drop (bar)	Whp (bara)	Cost Thousands US$
S1-C	122	760	-88	1520	0.8	6.00	6.52	34.1	0.52		805.6
C-705	18	550	-19	1500	0.3	6.52	6.58	29.6	1.06	7.58	319.6
C-B	104	50	0	1523	0.7	6.52	6.57	35.0	0.05		47.0
B-725	25	20	0	1421	0.3	6.57	6.64	37.2	0.07	6.64	11.6
B-A	79	360	-20	1556	0.6	6.57	7.06	37.4	0.49		338.4
A-714	65	15	-2	1377	0.5	7.06	7.08	33.6	0.02	7.00	12.1
A-716	14	370	-15	2386	0.35	7.06	7.68	34.8	0.62	7.68	235.7
S1-718	28	220	-24	1112	0.3	6.00	6.56	28.7	0.56	6.56	127.8
S1-719	42	130	0	1295	0.4	6.00	6.34	36.7	0.34	6.34	90.1
S1-E	70	450	0	1420	0.6	6.00	6.46	31.3	0.46		423
E-726	21	20	0	1642	0.35	6.46	6.50	33.5	0.04	6.46	12.7
E-D	49	110	0	1325	0.5	6.46	6.58	26.0	0.12		88.8
D-707	25	260	-29	1250	0.3	6.58	7.21	29.3	0.63	7.21	151.1
D-715	24	260	0	1404	0.3	6.58	7.35	34.9	0.77	7.35	151.1
S2-I	105	170	0	1692	0.8	6.00	6.12	34.7	0.12		180.2
I-701	36	50	0	1300	0.4	6.12	6.22	31.0	0.10	6.22	34.7
I-H	69	75	0	1897	0.6	6.12	6.18	34.6	0.06		79.5
H-713	9	530	-24	1731	0.25	6.18	7.09	27.7	0.91	7.09	275.6
H-G	60	380	-68	1921	0.7	6.18	6.37	30.3	0.19		402.8
G-720	9	30	-8	2236	0.25	6.37	6.45	38.6	0.08	6.45	15.6
G-F	51	690	-44	1866	0.7	6.37	6.95	32.9	0.58		648.6
F-709	29	50	0	2032	0.5	6.95	6.99	28.1	0.04	6.99	40.4
F-721	22	540	-39	1647	0.35	6.95	8.02	32.7	1.07	8.02	344.0
S2-727	12	60	0	1763	0.25	6.00	6.20	39.1	0.20	6.20	31.2
S2-K	43	350	-62	1748	0.5	6.00	6.49	38.8	0.49		282.5
K-712	10	15	0	2050	0.25	6.49	6.53	37.4	0.04	6.53	7.8
K-J	33	290	-16	1657	0.5	6.49	6.71	25.3	0.22		234
J-706	23	20	0	1650	0.35	6.71	6.76	35.6	0.05	6.76	12.7
J-711	10	330	-7	1672	0.25	6.71	7.33	26.9	0.62	7.33	171.6
S2-710	18	1170	-49	1336	0.3	6.00	7.82	26.4	1.82	7.82	679.8
Total length		**8325**	**Total cost of two-phase pipelines**								**6255.4**

5. PRELIMINARY DESIGN OF SEPARATORS

Geothermal separators are the kidneys of a geothermal steam production facility. Their function is to clean the steam of liquid and solid impurities. The proper sizing and selection of separators are to achieve high separator efficiency and trouble-free operation of a power plant.

In NE-Olkaria the pressures at the wellheads are lower than the corresponding water saturation pressure, and thus a mixture of steam and water enters the steam supply system. Problems will occur if geothermal water containing dissolved solids reaches equipment, such as turbines and control valves. The dissolved solids will precipitate during pressure drop and form deposits, causing further growth of the scaling which reduces turbine output and may cause turbine vibration. The optimal separator design is one where the separation process leads to steam quality, where all water containing dissolved solids is removed from the steam phase.

In most geothermal field developments throughout the world the separators have been of the vertical, centrifugal type. The alternative is to use the horizontal gravity separators which might possibly be just as suitable as the vertical type and would probably be more economical from the investment and operational standpoint (Ballzus et al., 1992). In the design for Northeast Olkaria the classical vertical, centrifugal separators will be considered.

The following description of a design approach for separators is based on a paper by Lazalde-Crabtree (1984). For more details refer to the paper. The theory, design parameters and recommendations discussed by Lazalde-Crabtree enable the design engineer to calculate the size of the equipment and to estimate its performance under several operating conditions.

When selecting a separator, there are several design parameters that should be taken into account. These are, among others :

1. Steam quality of the separated steam.
2. Steam pressure drop.
3. Facility of operation and cleaning.
4. Cost.

The discussion will be based on the so called Webre-type separators. They are simple (no moving parts that can be corroded or eroded). In the Webre cyclone, the steam first moves in a spiral pattern to the top and then changes direction by 180° to go down and out the bottom outlet. Since both the steam and the water outlets are at the bottom of the cyclone, piping layouts are simple. Their simplicity of operation has been proven in many liquid-dominated geothermal fields. This type of separator is very easy to clean. This is a fundamental item because the geothermal brine contains silica, among other chemicals, which is mainly responsible for scaling. It is recommended to schedule at least one general maintenance per year for wellhead separators. The outlet steam quality and efficiency are very high. The reported steam quality (dryness) has an average higher than 99.99% at Cerro Prieto, Mexico.

The performance of steam-water cyclones is governed by two types of variables :

1. Operating variables, relating to properties, rates and states of the phases. The mixture can be considered inside the separator at equilibrium, then all properties (pressure, temperature, density, viscosity, etc.) are fixed.
2. Design variables, relating to type and dimensions of cyclones. The outlet steam quality and the pressure drop are the main criteria for designing separators.

5.1 Design parameters

a) For separators, the inlet should be of the rectangular spiral type, and the floor of the spiral should have a slight fall, say 4°, just as it enters the cyclone to encourage the water to flow downwards more rapidly.

b) The steam outlet pipe should be as large as possible, even inside of the top head of the equipment. The only limitation is that the area between the end of this pipe (lip) and the wall of the top head should be at least equal to the cross-sectional area of the pipe. Lazalde-Crabtree (1984) recommends 1.25 times the cross-area. The diameter of this pipe, D_e, should be equal to the inlet pipe diameter, D_t.

c) The outlet water pipe diameter, D_b, should be equal to the inlet mixture pipe diam., D_t.

d) The separator should consider a water drum which can be either integrated or not. This drum acts as a volume to give smooth operation and as a water-seal to avoid steam losses.

Figure 23 shows the nomenclature used in the text with reference to separator design. The separator has spiral inlet with a change in cross-section from cylindrical to rectangular shape at the entrance.

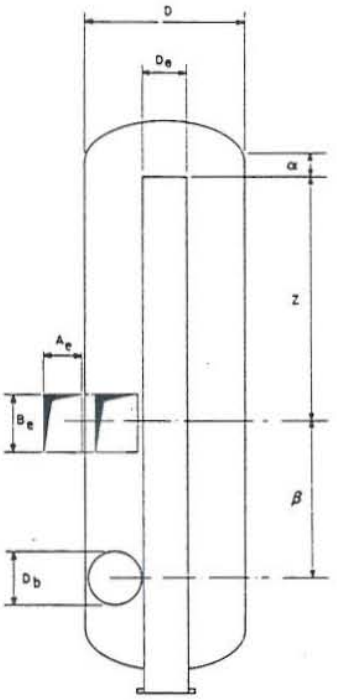

FIGURE 23: Steam-water separator

The recommended design parameters for geothermal separators are summarized in Table 6.

TABLE 6: Recommended design parameters for geothermal separators (Lazalde-Crabtree, 1984)

Parameter	Recommended value for separator design
Maximum steam velocity at inlet mixture pipe	45 m/s
Steam velocity range at inlet mixture pipe	25-40 m/s
Maximum annular upward steam velocity inside cyclone	4.5 m/s
Upward steam velocity inside cyclone	2.5-4.0 m/s
$R_1 = D/D_t$	3.3
$R_2 = D_e/D_t$	1.0
$R_3 = D_b/D_t$	1.0
$R_4 = \alpha/D_t$	-0.15
$R_5 = \beta/D_t$	3.5
$R_6 = z/D_t$	5.5

5.2 Efficiency of separation

There are two different terms that are very often indistinct:

1. The efficiency of separation, η_{ef}, defined as the mass ratio of separated liquid to inlet liquid.
2. The outlet steam quality, x_o, defined as the mass ratio of outlet steam to outlet steam-water.

By definition

$$\eta_{ef} = \frac{W_L - W_A}{W_L} \tag{25}$$

$$x_o = \frac{W_G}{W_G + W_A} \tag{26}$$

Subtituting Equation 25 into Equation 26, outlet steam quality is related to efficiency by

$$x_o = \frac{W_G/W_L}{1 - \eta_{ef} + W_G/W_L} \tag{27}$$

If $\eta_{ef} = 0$ then x_o is the inlet steam quality. If, on the other hand, $\eta_{ef} = 1$, then $x_o = \eta_{ef} = 1$ which is the only case where $x_o = \eta_{ef}$.

It has been shown (Lazalde-Crabtree, 1984) that outlet steam quality is low when the inlet steam velocity and the upward steam velocity (annular steam velocity inside of the separator) are low. When both steam velocities increase, the outlet steam quality goes up to a point (breakthrough point) where the outlet steam quality breaks down drastically. For modelling, it is assumed that there are two independent phenomena with influence on the efficiency of separation as follows:

$$\eta_{ef} = \eta_m \eta_A \tag{28}$$

where

η_m = centrifugal efficiency; and η_A = entrainment efficiency.

The centrifugal efficiency increases when the inlet steam velocity goes up ($\eta_m \to 1$ as $V_T \to \infty$), and the entrainment efficiency goes up when the upward annular steam velocity goes down ($\eta_A \to 1$ as $V_{AN} \to 0$). For more details about the correlations for the efficiency as defined by Lazalde-Crabtree (1984), refer to that paper.

5.3 Pressure drop

The steam pressure drop can be expressed as (Lazalde-Crabtree, 1984)

$$\Delta P = \frac{(NH)u^2 \rho_G}{2} \tag{29}$$

where

$$NH = 16\frac{A_e B_e}{D_e^2}; \qquad u = \frac{Q_G}{A_o}; \qquad Q_G = \frac{mx}{\rho_G}.$$

Q_G is the inlet steam volumetric flowrate expressed as $A_o = A_e B_e$

The total pressure drop can be split into two parts (Lazalde-Crabtree, 1984)

$$\Delta P = \Delta P_1 + \Delta P_2 \tag{30}$$

ΔP_1 is the steam pressure drop between the separator inlet and the separator body, and ΔP_2 between the separator body and the separator steam outlet.

$$\frac{\Delta P_1}{\Delta P} \approx 0.6 \qquad \frac{\Delta P_2}{\Delta P} \approx 0.4 \tag{31}$$

5.4 Sizing and cost of separators

The separation pressure that has been used in the design of separators was selected on the basis of optimization of separation pressure for the reservoir temperatures (Figure 24, Jonsson, 1976). From the chemical composition of discharge from Northeast Olkaria wells (Table 1) the saturation temperature for the separation pressure of 6 bara was compared with the Opal (silica) saturation temperature. The following equation (Fournier, 1989) has been used to calculate the silica saturation temperature:

$$\log S = [-731/T] + 4.52 \tag{32}$$

where S is the concentration of dissolved silica in mg/kg and T is temperature in degrees Kelvin. Using silica concentrations given in Table 1 we obtain the silica saturation temperature of 148°C. This is lower than the saturation temperure for a pressure of 6 bara, 158.2°C.

The two separation stations should have adequate capacity to separate sufficient steam to supply a 64 MW_e power plant. The total specific steam consumption (including steam ejector requirements) in kg/MW_e that has been assumed is the one suggested in the Feasibility Study report (Ewbank Preece - Virkir, 1989). Therefore, a value of 2.29 kg/MW_e has been used to estimate the total power station steam requirement. Two separation stations have been proposed and each will supply steam to operate one of the two 32 MW_e turbine-generators to be installed at the NE-Olkaria power plant. Each separator station should therefore provide 73.28 kg/s.

An illustrative example will be given based on the sizing of the separators to be installed at separator station S1 (Figure 18). The separator, s, should be designed to give an outlet steam quality of 99.95 % for the following conditions:

Mixture enthalpy	= 1414 kJ/kg;
Separation pressure	= 6 bara;
Two-phase mixture flux	= 206 kg/s ;
Maximum pressure drop	= 0.5 bar;

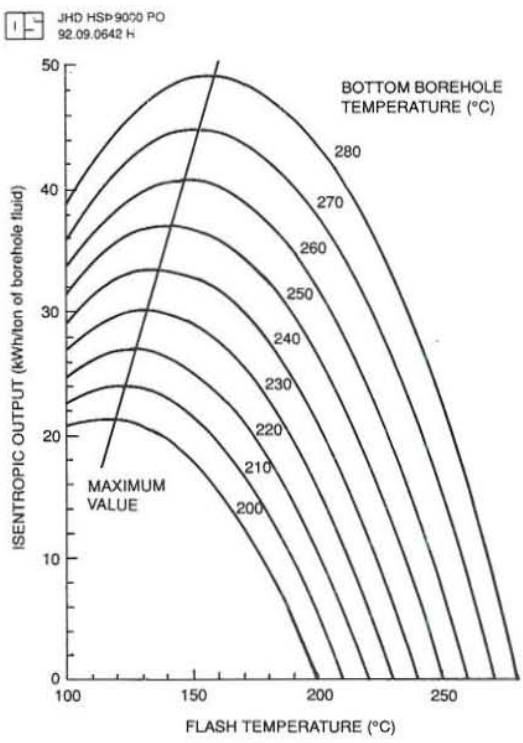

FIGURE 24: Optimization of separation pressure

a) Preliminary calculations
With the separation pressure and steam tables we can obtain all thermodynamic and hydrodynamic properties. The mixture inlet quality is 0.36.

b) Design
Inlet area and diam. of inlet pipe (assuming the inlet velocity, 25 m/s) based on Table 6:
Inlet diameter, D_t = 1.1 m

Table 6 gives:

D	= 3.63 m
D_e	= 1.1 m
D_b	= 1.1 m
α	= -0.165 m
β	= 3.85 m
z	= 6.05 m

The separator has a spiral inlet with a cross-sectional area, A_o = 1.21 m^2

c) Centrifugal efficiency, η_m = 98.767%

d) Entrainment efficiency, η_A = 99.999%

e) Efficiency, η = 98.766%

f) Outlet steam quality, x_o = 97.82%

g) Pressure drop, ΔP = 9.8 kPa

Even though ΔP is lower than 50 kPa, x_o is less than 99.95%. Therefore, the designed separator cannot achieve its task.

Consequently, the inlet steam velocity was changed to 35 m/s but the steam quality, x_o, only went up by 1% to 98.8%. According to the recommendations given in Table 6 with these inlet velocities for steam, the steam quality obtainable should be higher. This descrepancy suggests that smaller units with combined separation capacity equivalent to that of a large single one might be a good idea. Smaller units are also operationally convenient especially in cases of breakdowns.

The cases of utilizing two, three and four smaller units have been considered. The variation in the cost of the separation plant S1 as the number of separation units increases from one to four is given in Appendix III. The cost estimates were carried out with the aid of computer facilities and latest cost data available at VGK consulting engineers, Iceland.

5.5 The total cost

Considering four separator units per separation station each of separation capacity for steam equivalent to 10 MW_e (or 18.5 kg/s of steam) and using the cost figures from Appendix III for inlet velocity of steam equal to 25 m/s, we can calculate the cost of the two separation stations. It comes to

2.6655 M USD

6. PRELIMINARY SIZING OF REINJECTION PUMPS

A sump pit will be constructed for the reinjection pumps beside the main road as shown in Figure 18. The waste water from each separation station discharge pond will flow to the reinjection sump pit using only gravity head from a decanting overflow inlet at each pond. A simple level control valve at each cooling tower basin will pass a blowdown flow, utilizing gravity head, from the cooling tower inlet pipe to the reinjection sump. An overflow pond would be provided alongside the reinjection sump to allow for periods of pump failure.

With a separation pressure of 6 bara and a turbine steam requirement of 147 kg/s per 64 MW_e, the water fraction in the separation stations will be:

Separation station S1	= 69 kg/s at 1674 kJ/kg
Separation station S2	= 116 kg/s at 1414 kJ/kg
Blowdown from the cooling towers	= 42 kg/s (Ewbank Preece - Virkir, 1989)

Therefore, the maximum design water flows requiring disposal are 227 kg/s.

Static head change	= 164 m
Pipeline effective length	= 2320 m
Pipeline diameter	= 400m

6.1 Sizing and cost of pumps

With the reinjection well selected to be OW-704 the pumping requirements from the reinjection sump have been assessed using the following equation:

$$W_P = \frac{m_f \Delta P 100}{\rho_L \eta} \qquad (33)$$

where

W_P = power requirement, kW;
m_f = water flowrate, kg/s;
ΔP = total pressure head, bar;
η = pump efficiency.

Using the values listed in Chapter 6 and assuming pump efficiency of 75%, the pump requirements are 500 kW.

For operational reasons it is safer and more convenient to have two pumps of capacity 250 kW each, instead of one of capacity 500 kW. Due to the chemical nature of the brine it is expected that these pumps will require special maintenance programmes. It is, therefore, reasonable to have two pumps in operation and two on standby. Therefore, the costs will be made with regard to four complete pumps (including motor) of capacity 250 kW.

The cost can be based on data provided by VGK consulting engineers regarding the price of cold water pumps at Nesjavellir geothermal field, Iceland. To that figure 20% has been added to take care of special requirements for brine, giving:

The cost per unit = 68,000 USD;

The total cost of four (4) pumps, each 250 kW = 272,000 USD.

7. RESULTS

7.1 Discussion

In the pipeline lay-out, alternative routes are possible as indicated in Figure 18. For instance the two-phase mixture from OW-709 and OW-721 could be hooked to the flow from OW-721 instead of hooking it to flow from OW-720. This would modify the pipe sizing and therefore the costs accordingly. This has not been investigated in this study.

The cost distribution as expressed in Figure 22 has a large component of costs for labour charge. The cost of labour in Kenya is lower than that in Iceland and hence the costs will be lower in Kenya. Also, it does not include the costs of valves and other associated safety devices. The costs would be increased if these were to be considered.

In the separation stations, the cost of a steam vent has not been considered. Neither have the costs of the discharge ponds, the reinjection sump pit and the open drains been included, nor the cost of design and civil works.

7.2 Conclusions

Preliminary design for the steam gathering system to be constructed at Northeast Olkaria has been conducted. The sizing of major equipment that constitute the system has been done. The operational wellhead pressures are known from the output curves. The study has shown that it is possible to design a central separation system for utilizing the steam from the field. The total cost of the equipment required for the gathering system has been estimated at 13.25 M USD.

ACKNOWLEDGEMENTS

The author is grateful to Dr. Ingvar B. Fridleifsson, director of UNU Geothermal Training Programme, for availing the facilities required for carrying out this study. He is most indebted to Dr. Arni Ragnarsson for the wonderful guidance while carrying out this project. Not to forget Sverrir Thorhallsson and Grimur Björnsson for helping to edit this report. Special thanks should also go to Ludvik Georgsson and all members of staff at Orkustofnun who were so helpful. He is also thankful to the management of Kenya Power Company Ltd. for providing the data used.

REFERENCES

Arnorsson, S., Bjornsson, S., Muna, Z.W., and Ojiambo, S.B., 1990: The use of gas chemistry to evaluate boiling processes and initial steam fraction in geothermal reservoirs with an example from the Olkaria field, Kenya. Geothermics, vol. 19, 6, 497-514.

Arusei, M.C., 1991: Hydrochemistry of Olkaria and Eburru geothermal fields, Kenyan Rift Valley. UNU Geothermal Training Programme, Iceland, report 2, 40 pp.

Ballzus, C., Karlsson, T., and Maack, R., 1992: Design of geothermal steam supply systems in Iceland. Transactions of the International Conference on Industrial Uses of Geothermal Energy, Reykjavik, Iceland, 2-4 September 1992, 8 pp.

Ewbank Preece - Virkir, 1989: Feasibility study for a geothermal power station at Northeast Olkaria. Report prepared for the Kenya Power Company Ltd.

Fournier, R.O., 1989: Lectures on geochemical interpretation of hydrothermal waters. UNU Geothermal Training Programme, Iceland, report 10, 73 pp.

Freeston, D.H., 1982: Lectures on geothermal energy developments in New Zealand. UNU Geothermal Training Programme, Iceland, report 12, 108 pp.

Hewitt, G.F., 1982: Pressure drop. In: Hetsroni, G. (editor): Handbook of multiphase systems. McGraw Hill, 2.44-2.75.

Jonsson, V.K., 1976: Geothermal power utilization, present and future. In: Editor Hartnett, J.P.: Alternative energy sources. Academic Press, New York, 279-324.

Lazalde-Crabtree, H., 1984: Design approach of steam-water separators and steam dryers for geothermal applications. GRC bulletin, September 1984, 11-20.

Merz and McLellan - Virkir, 1986: Olkaria Geothermal Project, status report on steam production, November, 1986. Report prepared for the Kenya Power Company Ltd.

Ouma, P., 1992: Performance of East Olkaria geothermal field during ten years of production. Transactions of the International Conference on Industrial Uses of Geothermal Energy, Reykjavik, Iceland, 2-4 September 1992, 10 pp.

APPENDIX I: Output curves for selected wells in NE-Olkaria field

OW701

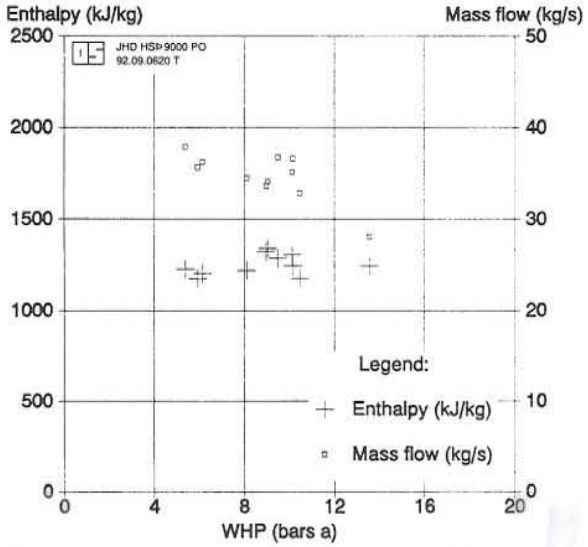

OW705

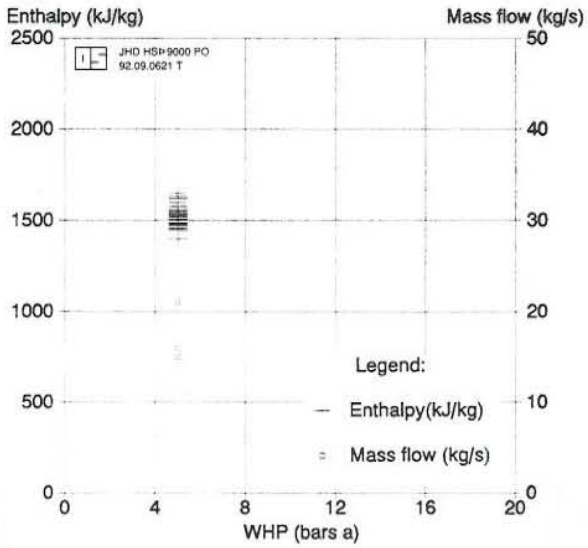

OW706

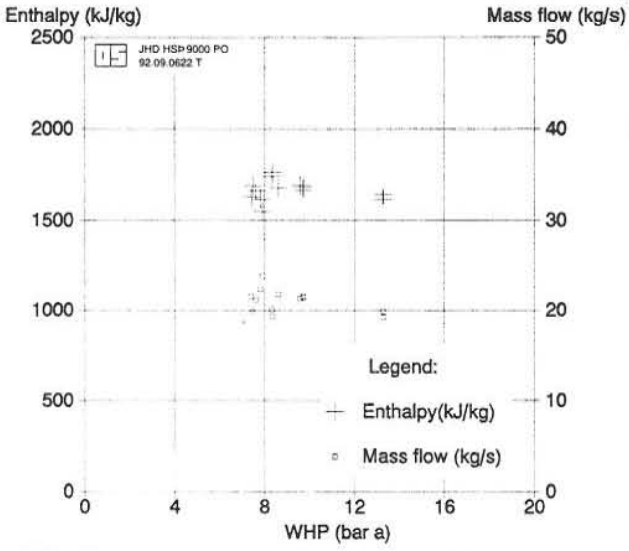

OW707

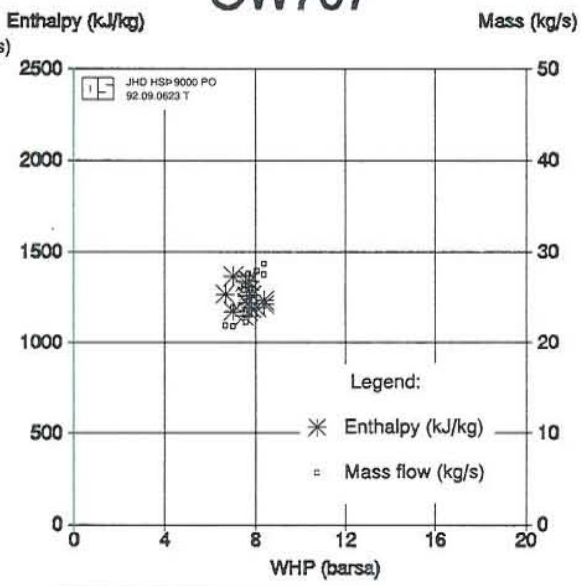

OW709

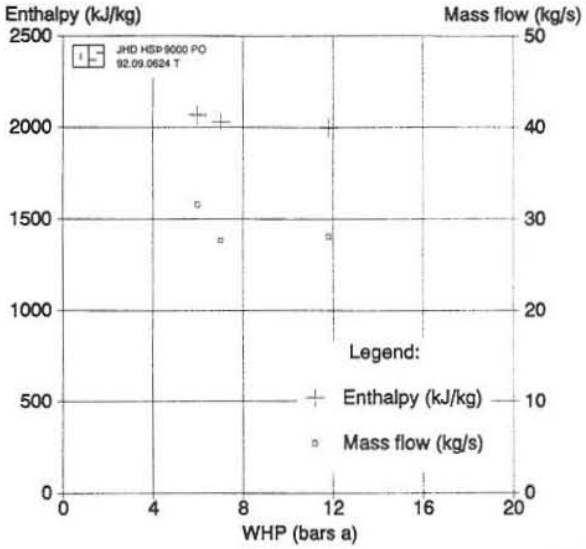

OW710

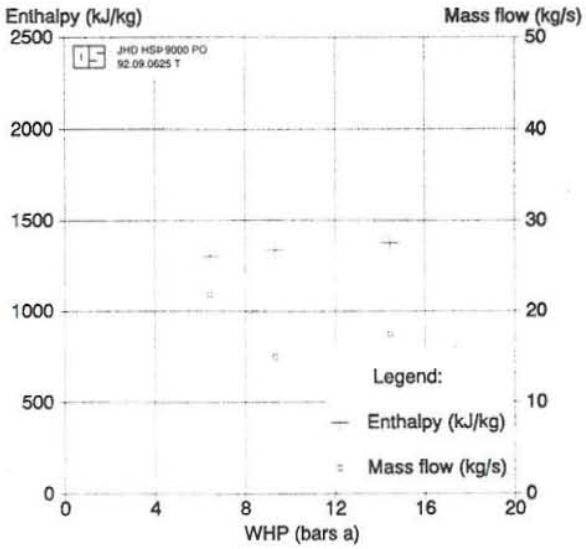

OW711

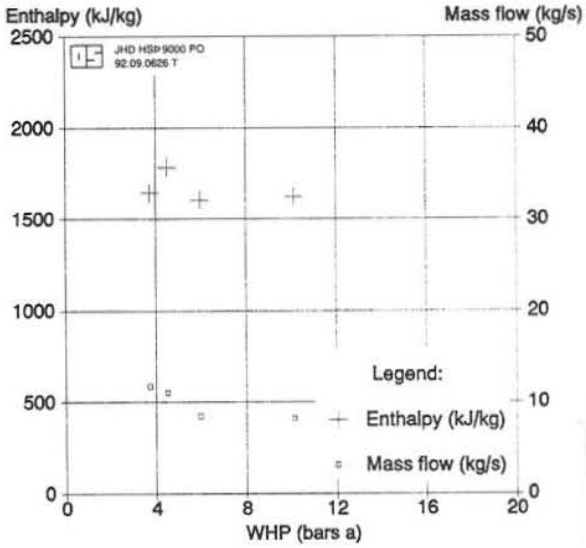

OW712

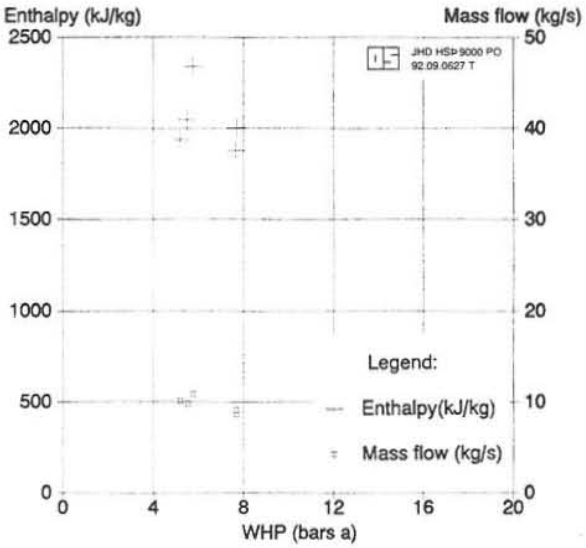

OW713

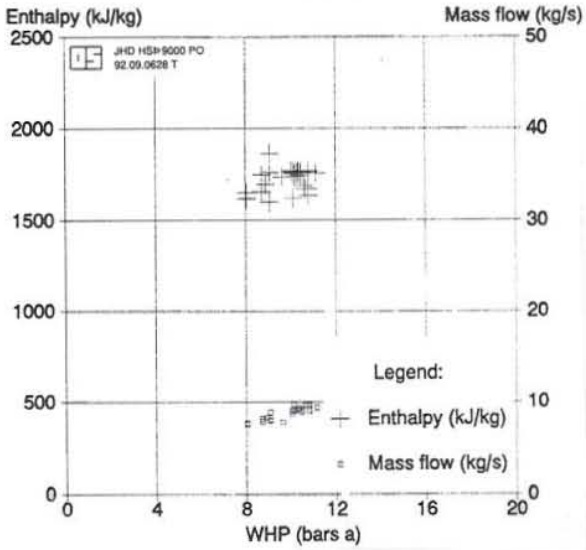

OW714

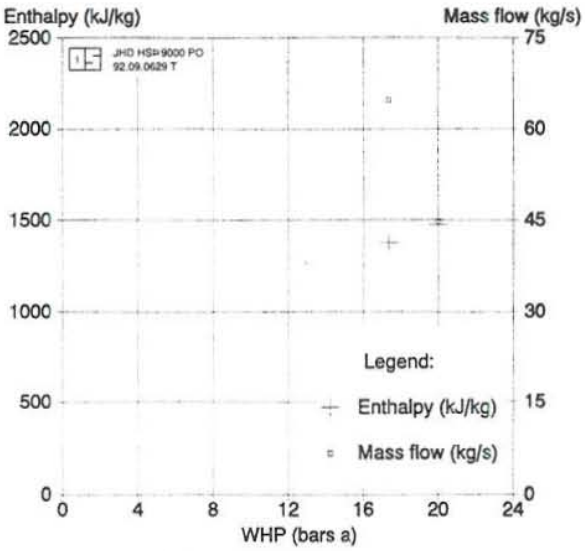

OW715

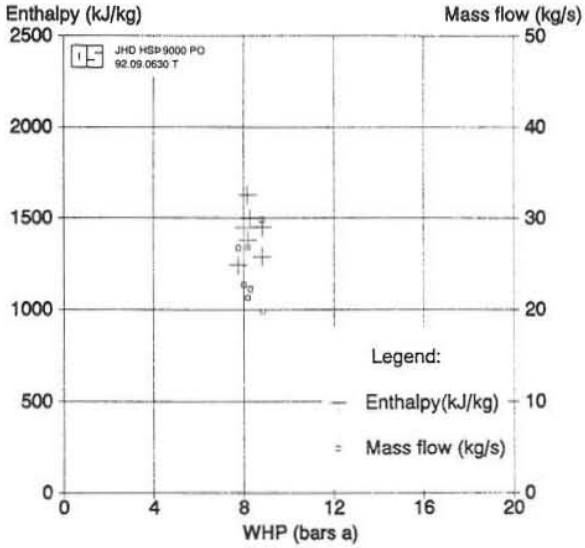

OW716

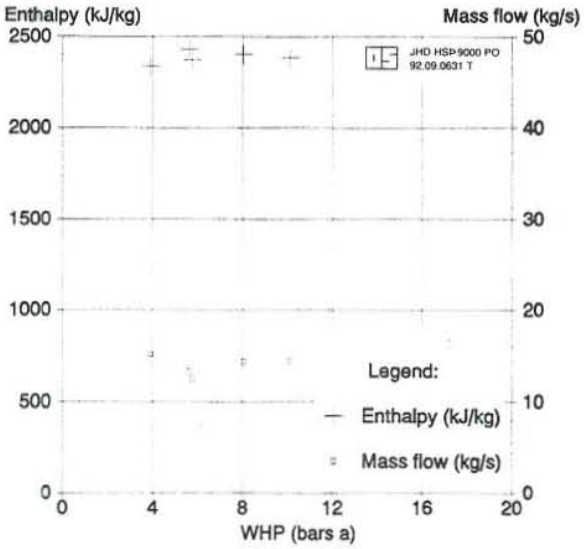

OW718

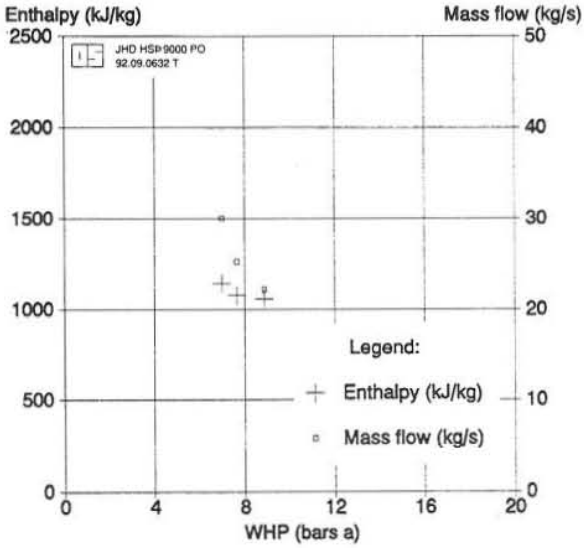

OW719

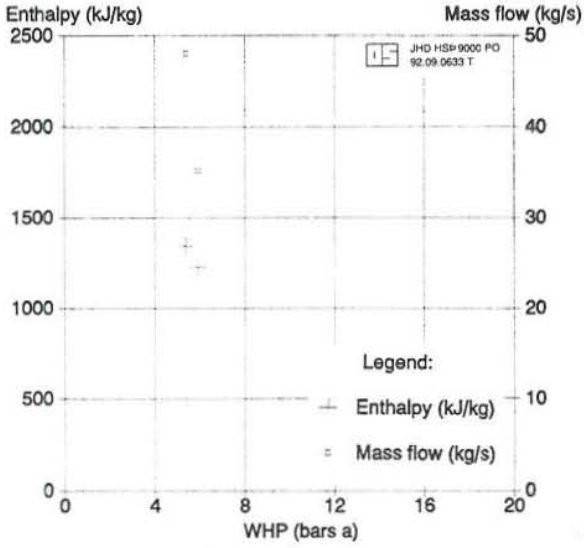

OW720

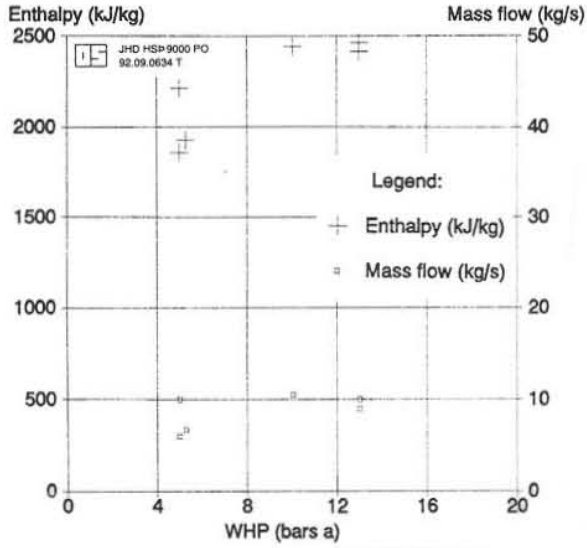

OW721

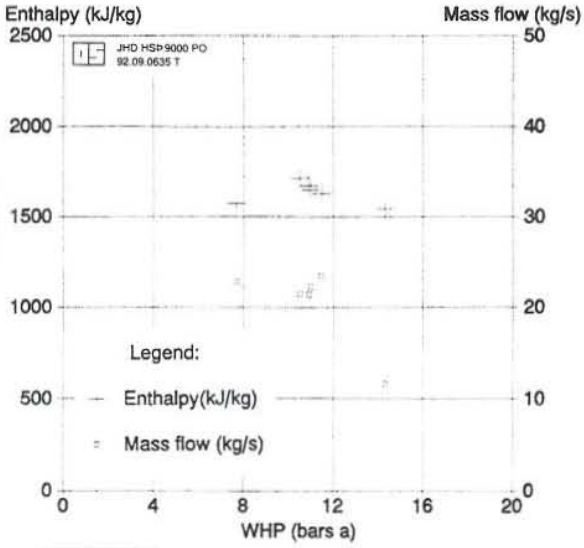

OW725

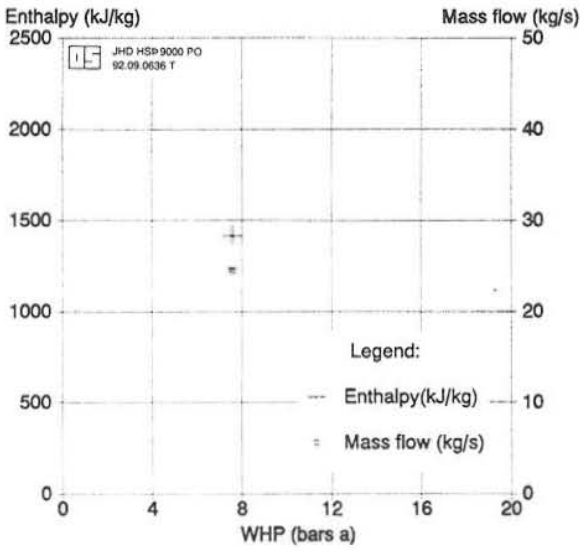

OW726

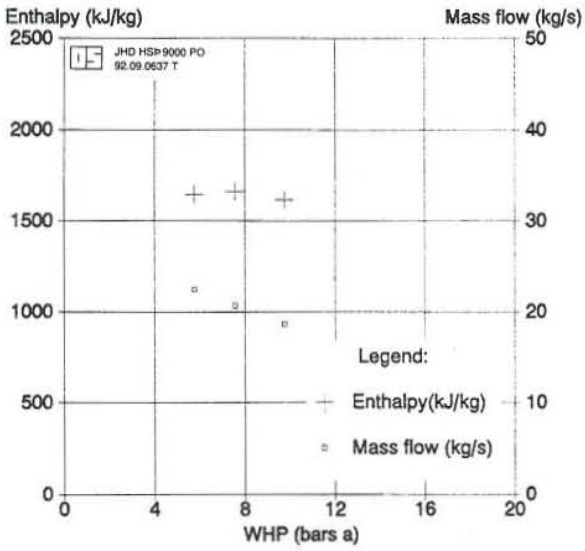

OW727

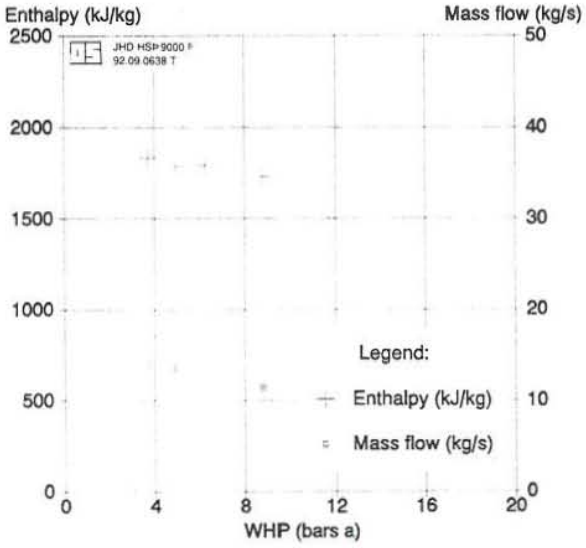

APPENDIX II: Computer print-outs for two-phase pressure drop calculations

UNU
15. sept 1992

TWO PHASE CALCULATOR - dP

Pipeline for 710

LINE IDENTFN.	DIA. (m)	LENGTH (m)	ROUGHN (m)	FLOW kg/s	PRESS bar a	RRATIO	Ht kJ/kg	Hf kJ/kg
S2-710	0.3396	1170	0.0001	18	6.00	0.00029	1336	670.42

H.VAP kJ/kg	SPV.WAT m3/kg	SPV.VAP m3/kg	LIQ.VIS N s/m2	VAP.VIS N s/m2	SURFTEN N/m	DRYNESS	
2085.00	0.001101	0.315495	0.000169	0.000014	0.046858	0.319	0.0224

	L.M.MUL	VAP.VELS m/s	ReNo.	FRIC.FAC f	PRES.DR Pa	B(X) m/s	B(Y) m/s
	0.14957	4.377	20.0	1.5e+06	0.0156	149148	3.0	2.6

W.H.P at OW-710 (bara) = 7.49

```
**********************************************************************

PRESSURE DROP IN A PIPELINE (WATER/STEAM)

**********************************************************************

Water(w), steam(s) or two-phase(t) flow                 :    t
Given inlet(i) or outlet(o) conditions                  :    o
Nominal pipe diameter                          (mm)     :  350.0
Pipe length                                    (km)     :    1.17
Roughness factor                               (mm)     :    0.1
Outlet pressure                                (bara)   :    6.0
Mass flow                                      (kg/s)   :   18.0
Elevation shift                                (m)      :  -49.0
Calculation step length                        (m)      :  100.0
Pressure drop in bends etc.                    (%)      :   15.0
Total enthalpy                                 (kJ/kg)  : 1336.0
Two-phase model:  L-M:(1) Friedel:(2)                   :    2.0


                                          Inlet              Outlet

Pressure (bar a)                          7.197              6.000
Mass flow (kg/s)                         18.000             18.000
Temperature (C)                         166.079            158.838
Total enthalpy (kJ/kg)                 1336.000           1336.000
Steam fraction                             .308               .319
Steam density (kg/m3)                     3.765              3.170
Water density (kg/m3)                   901.253            908.380
Mixture density (kg/m3)                  12.112              9.857
Void fraction                              .898               .910
Water velocity (m/s)                      1.494              1.646
Steam velocity (m/s)                     18.104             22.003
Slip factor                              12.121             13.365
Bakers parameter Bx                       3.580              3.058
Bakers parameter By                       2.271              2.555

Total pressure drop (bar a)               1.197
Frictional pressure drop (bar a)          1.247  (104.126 %)
Accelerational pressure drop (bar a)       .004  (   .297 %)
Gravitational pressure drop (bar a)       -.053  ( -4.423 %)
Inside pipe diameter (mm)               339.600
```

APPENDIX III: Variation in costs for separator plant S1 with increase in separator units

SEPERATOR STATION 10.10.1992
COST ESTIMATION VGK/EJ
[NV244/OLKARIA.WQ1]

(Exhaust system, design and tax not included)

DESIGN CRITERIA, EAST OLKARIA FIELD

Pressure class	16	PN	
Operating pressure	6	bara	
Mg	74	kg/s	1 USD = 56 íkr
Mf (x=0,36)	130	kg/s	
vg	0,31546	m3/kg	
Vg	23,3	m3/s	
Vinlet	20	m/s	

VERTICAL SEPERATORS, DIMENSIONS, REF. BANGMA

Number of separators	1	2	3	4
D-inlet calc. [mm]	1219	862	704	610
D-sep (3D) [mm]	3657	2586	2111	1829
L-sep (11,5D) [mm]	14019	9913	8094	7010
t-sep [mm]	20	15	13	11
Weight-sep [kg/sep]	46208	17007	9537	6348
Weight-sep total [kg]	46208	34013	28611	25391
Relative tot. weight	1,00	0,74	0,62	0,55
D-steam valves [mm]	900	600	500	400
D-brine valves [mm]	400	300	250	200

COST CALCULATIONS [TH. íKR]

Seperator cost/unit				
Steel material	3.466	1.276	715	476
Steel work	15.017	5.527	3.100	2.063
Insul./sheat. material	507	253	169	127
Insul./sheat. work	1.231	812	637	536
Total/unit	20.221	7.868	4.620	3.202
Seperator cost, total				
Steel material	3.466	2.551	2.146	1.904
Steel work	15.017	11.054	9.299	8.252
Insul./sheat. material	507	507	507	507
Insul./sheat. work	1.231	1.624	1.910	2.143
Seperators, total	20.221	15.736	13.861	12.806
Pipes and valves				
Steel material /valves	12.787	12.307	12.631	14.002
Steel work	3.450	5.254	7.501	9.015
Insul./sheat. material	755	945	1.075	1.323
Insul./sheat. work	1.211	1.658	1.986	2.656
Pipes and valves, total	18.203	20.164	23.193	26.996
Steel supports, ladders and steelfloors, total	9.102	10.082	11.597	13.498
Earth work and foundations, total	9.000	10.000	11.000	12.000
Miscellaneous 20%	11.305	11.197	11.930	13.060
TOTAL [íKR]	67.830	67.179	71.581	78.360

SEPERATOR STATION 10.10.1992
COST ESTIMATION VGK/EJ
[NV244/OLKARIA.WQ1]

(Exhaust system, design and tax not included)

DESIGN CRITERIA, EAST OLKARIA FIELD

Pressure class	16	PN	
Operating pressure	6	bara	
Mg	74	kg/s	1 USD = 56 íkr
Mf (x=0,36)	130	kg/s	
vg	0,31546	m3/kg	
Vg	23,3	m3/s	
Vinlet	25	m/s	

VERTICAL SEPERATORS, DIMENSIONS, REF. BANGMA

Number of separators	1	2	3	4
D-inlet calc. [mm]	1090	771	630	545
D-sep (3D) [mm]	3271	2313	1889	1636
L-sep (11,5D) [mm]	12539	8867	7240	6270
t-sep [mm]	18	14	11	10
Weight-sep [kg/sep]	33450	12362	6953	4639
Weight-sep total [kg]	33450	24724	20859	18554
Relative tot. weight	1,00	0,74	0,62	0,55
D-steam valves [mm]	900	600	500	400
D-brine valves [mm]	400	300	250	200

COST CALCULATIONS [TH. íKR]

Seperator cost/unit				
Steel material	2.509	927	521	348
Steel work	10.871	4.018	2.260	1.508
Insul./sheat. material	405	203	135	101
Insul./sheat. work	1.077	710	557	469
Total/unit	14.862	5.858	3.473	2.425
Seperator cost, total				
Steel material	2.509	1.854	1.564	1.392
Steel work	10.871	8.035	6.779	6.030
Insul./sheat. material	405	405	405	405
Insul./sheat. work	1.077	1.421	1.671	1.875
Seperators, total	14.862	11.716	10.420	9.702
Pipes and valves				
Steel material /valves	12.787	12.307	12.631	14.002
Steel work	3.450	5.254	7.501	9.015
Insul./sheat. material	755	945	1.075	1.323
Insul./sheat. work	1.211	1.658	1.986	2.656
Pipes and valves, total	18.203	20.164	23.193	26.996
Steel supports, ladders and steelfloors, total	9.102	10.082	11.597	13.498
Earth work and foundations, total	9.000	10.000	11.000	12.000
Miscellaneous 20%	10.233	10.392	11.242	12.439
TOTAL [íKR]	61.400	62.355	67.451	74.635

SEPERATOR STATION
COST ESTIMATION

10.10.1992
VGK/EJ
[NV244/OLKARIA.WQ1]

(Exhaust system, design and tax not included)

DESIGN CRITERIA, EAST OLKARIA FIELD

Pressure class	16	PN	
Operating pressure	6	bara	
Mg	74	kg/s	1 USD = 56 fkr
Mf (x=0,36)	130	kg/s	
vg	0,31546	m3/kg	
Vg	23,3	m3/s	
Vinlet	35	m/s	

VERTICAL SEPERATORS, DIMENSIONS, REF. BANGMA

Number of separators	1	2	3	4
D-inlet calc. [mm]	922	652	532	461
D-sep (3D) [mm]	2765	1955	1596	1382
L-sep (11,5D) [mm]	10598	7494	6119	5299
t-sep [mm]	16	12	10	9
Weight-sep [kg/sep]	20598	7665	4332	2901
Weight-sep total [kg]	20598	15330	12997	11606
Relative tot. weight	1,00	0,74	0,63	0,56
D-steam valves [mm]	900	600	500	400
D-brine valves [mm]	400	300	250	200

COST CALCULATIONS [TH. fKR]

Seperator cost/unit				
Steel material	1.545	575	325	218
Steel work	6.694	2.491	1.408	943
Insul./sheat. material	290	145	97	72
Insul./sheat. work	880	580	455	383
Total/unit	9.408	3.791	2.285	1.616
Seperator cost, total				
Steel material	1.545	1.150	975	870
Steel work	6.694	4.982	4.224	3.772
Insul./sheat. material	290	290	290	290
Insul./sheat. work	880	1.161	1.365	1.532
Seperators, total	9.408	7.583	6.854	6.464
Pipes and valves				
Steel material /valves	12.787	12.307	12.631	14.002
Steel work	3.450	5.254	7.561	9.015
Insul./sheat. material	755	945	1.075	1.323
Insul./sheat. work	1.211	1.658	1.986	2.656
Steel supports, ladders and steelfloors, total	9.102	10.082	11.597	13.498
Earth work and foundations, total	9.000	10.000	11.000	12.000
Miscellaneous 20%	9.143	9.566	10.529	11.792
TOTAL [fKR]	54.856	57.395	63.172	70.749